SEAKEEPING STUDY OF TWO OFFSHORE WIND TURBINE PLATFORMS

Treball Final de Grau

Facultat de Nàutica de Barcelona
Universitat Politècnica de Catalunya

Treball realitzat per:
Ana Barcos Latorre

Dirigit per:
Julio García Espinosa

Grau en GSTN

Barcelona, dimecres 09 de juliol del 2014

Departament de CEN

UNIVERSITAT POLITÈCNICA DE CATALUNYA
BARCELONATECH
Facultat de Nàutica de Barcelona

Acknowledgement

I would like to express my gratitude and appreciation to all those who gave me the possibility to do this project.

A special thanks to the head of the project, Prof. Julio García Espinosa, Ph.D, whose help, patience and encouragement helped me to keep the progress in track.

I would also like to acknowledge with much appreciation the crucial role of my family and friends who have always given much support to me.

Motivation

Nowadays renewable energies have become a trend in topic in every energetic talk or written article. The global awareness for the need of transition to a lower carbon energy system plus the whole pernicious effects of carbon dioxide (CO2) and the greenhouse gas (GHG) on the ozone layer, makes realize that every low carbon technological innovations are essential to achieve the world wide targets set (like for example on the UN Kyoto Protocol [1]). Being renewable energies the only ones which can face up both challenges.

Currently massive offshore renewable energies research projects are ongoing. Not only is the ocean a vast energy container source, it also covers around 70% of the earth surface. Despite being many ways of harvesting this energy, wind power is the one most desired due to its high performance rate or efficiency (≈60%) compared with any other renewable source, its low maintenance[2] and its low cost-production ratio[3].

Development of these devices goes through several steps between the initial concept and the commercial product (see Figure 1) which are performed in many full scale ocean energy test centres constructed all over the world.

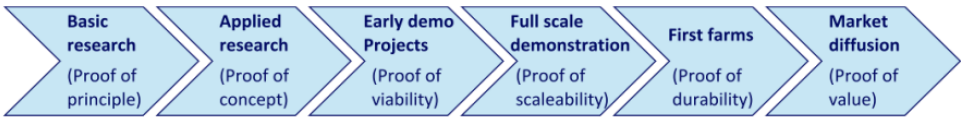

Figure 1. The Technology Journey

Source: http://si-ocean.eu/en/upload/docs/WP3/Technology%20Status%20Report_FV.pdf

Knowledge, technology and experience from other industry sectors converge in the wind offshore energy production process providing a basis for its quick development and playing a very important role in its steps towards commercial viability.

- **From wind industry**: much work has been completed regarding to computational turbine models and resource assessment.
- **From shipping**: many aspects related to the marine environment survivability like corrosion prevention techniques or anti-fouling coatings; as well as, mooring and foundation's notions, plus many other aspects, represent further areas of know-how that the shipping industry contributes to the ocean energy sector.

But the drive for accelerated change can also present unrealistic short-term expectations. Concurrently, the requirement for accelerated development and deployment presents a very serious technical and financial challenge. The uncertainties that exist within the ocean energy sector need to be understood. What gives its uppermost importance to the development of robust techniques with the purpose of solving the problems associated with the environment and in particular to the wave's effects towards the whole structure and its mooring.

Abstract

This project involves the modelling and seakeeping study of 2 offshore wind platforms. They are in fact; the Tension Leg Platform (TLP) studied in the D. Matha thesis and the floating platform studied in the IEA Offshore Code Comparison Collaboration (OC3) –Phase IV Hywind Spar-Buoy –. Both of them were developed specifically to support the rotor, nacelle and tower of the National Renewable Energy Laboratory (NREL) baseline 5MW system (see Figure 2).

These structures are modelled and calculated with the SeaFEM program.

To validate each generated structure, the Response Amplitude Operator (RAO) is going to be used as being itself the most popularized graphic which describes the structure natural frequencies in an appropriate way. This is the reason why RAOs operators become an important and characteristic parameter for the entire geometry.

Once all models have been properly created; a Jonswap wave spectrum is created and both linearized and non-linearized moorings are modelled in order to contrast:

- The body displacements from each structure (between linearized and non-linearized mooring system).
- The forces resulting to the platforms due to its mooring lines (with the non-linearized lines).

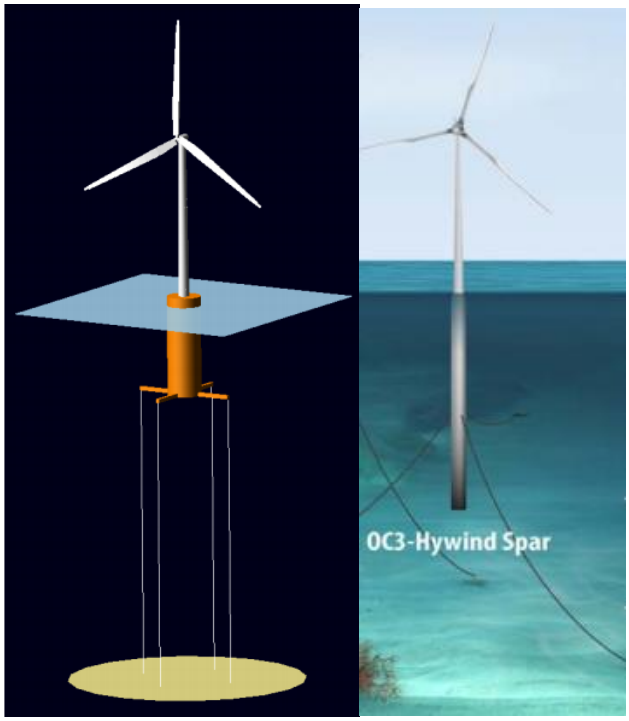

Figure 2. TLP, DeepCwind and Hywind Spar

Source: http://www.nrel.gov/docs/fy10osti/45891.pdf and http://www.nachhaltigwirtschaften.at/iea_pdf/reports/iea_wind_annual_report_2012.pdf

The report opens with a brief introduction to the offshore wind power in Chapter 1.

Once the introduction to the floating offshore wind platforms has been made, the Numerical models creation and the validation of the structures are presented in Chapter 2. The very first part of Chapter 2 – Chapter 2.1 – some general numerical data properties is explained. In Chapter 2.2; The NREL baseline 5MW system used in every studied platform is introduced, which is followed by Chapter 2.3 examining the TLP creation process. Chapter 2.4 displays the Hywind Spar-Buoy creation. RAO results analyses are presented at the lasts parts of each chapter for both floating structures.

In Chapter 3, the Jonswap wave spectrum is introduced to the programed platforms and all mooring lines study is done. Some general properties for both study platforms are introduced in Chapter 3.1. Chapters 3.2 and 3.3 show the differences between the linear and non-linear mooring lines study results obtained for TLP and Hywind Spar-Buoy. And Chapter 3.4 Introduces the mooring forces produced to the floating structures.

Finally, the conclusions are presented in Chapter 4.

Contents

Figures list

Tables list

Chapter 1. Offshore wind power.

In recent times wind energy electricity production capacity has been increasing substantially. As an example, in 2008, world's wind energy volume was actually approaching 1% of the global electricity production. Furthermore, in the next 20 years the percentage is estimated to be increased even more by means of offshore wind technology/ies development.

1.1. Offshore vs onshore wind turbines

Why offshore and not onshore wind turbines? Installing offshore wind turbines has more than a few advantages over onshore development (see Table 1).

	OFFSHORE	ONSHORE
Transport large elements	It takes the advantage of the high capacity of marine shipping and handling equipment.	It can present many difficulties due to the limited length which can be carried together with its isolated emplacements due to many siting issues (visual and noise impacts).
Wind (see Figure 3)	Wind blows faster and more smoothly at sea which allows producing more electricity per square meter of swept rotor area.	The slower and intermittent wind blowing makes larger rotor diameters to become necessary in order to produce the same power as an offshore installation would.
Energy transmission	Wind farms can be nearer to shore cities, which means, rather shorter transmission lines even being far enough to reduce visual and noise impacts.	Larger wind farms tend to be in fairly distant areas due to various sitting issues, such as visual and noise impacts, which can limit the number of acceptable locations for wind parks. Electricity must be transmitted over long power lines to cities.

Table1. Offshore vs Onshore wind turbines

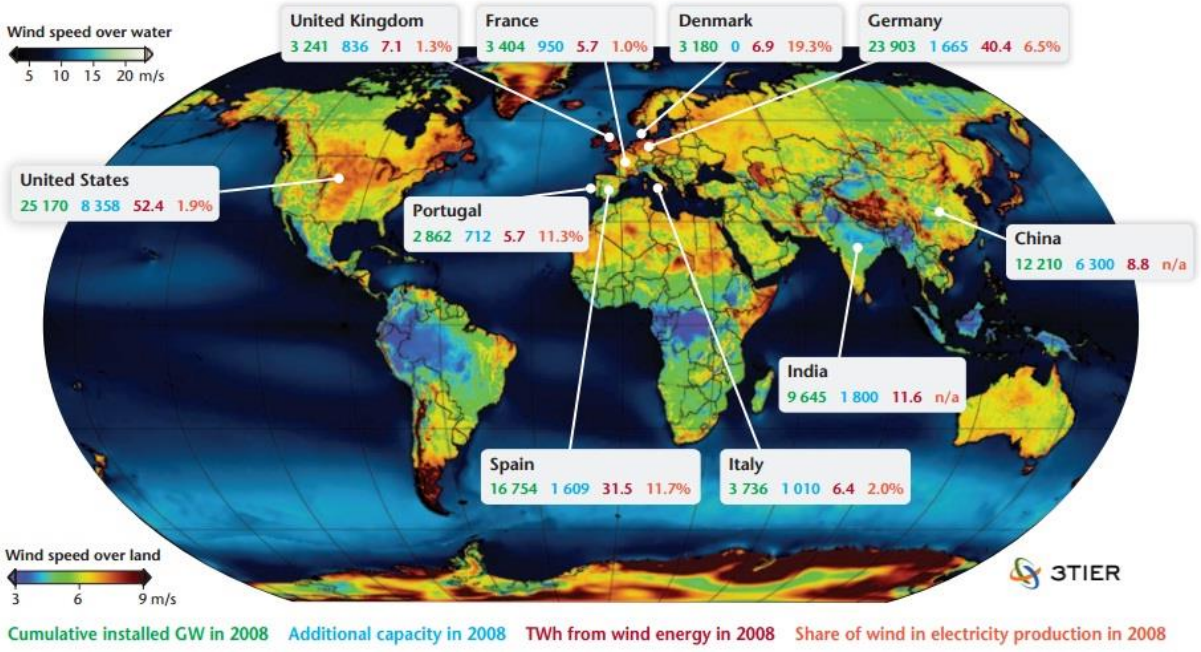

Figure 3. Global wind distribution with the installed capacity and production data for leading countries (at 80m height and 15km resolution)

Source: http://re.buildingefficiency.info/en/renewable-energy-technologies/wind/

1.2. Deep sea floating platforms

Currently offshore wind energy is moving into deeper waters, where floating platforms seem to be the most appropriate solution, as being there where wind currents are stronger. For that ambition, many floating platforms have been designed and tested like the semi-submergible, the barge, the spar and the TLP (see Figure 4), which are the most popular ones.

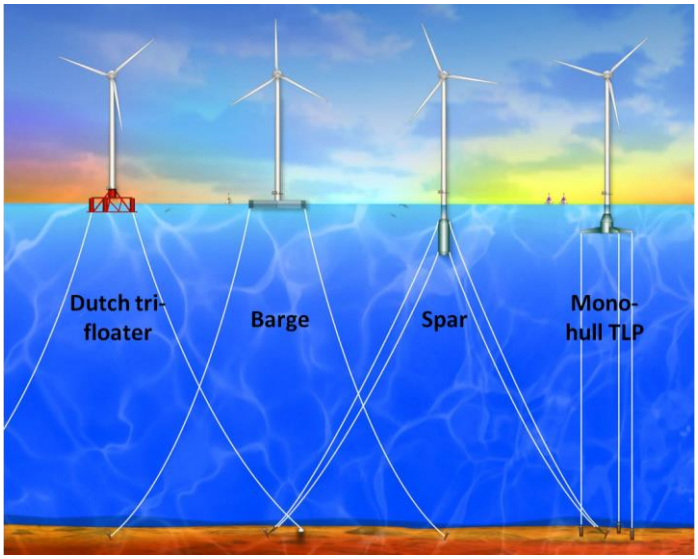

Figure 4. Deep sea floating platforms

Source: http://fessrg.ucsd.edu/Research/Wind/

Some of its uses, advantages and disadvantages are listed in the table below (see Table 2).

Structure	Uses	Advantages	Disadvantages
Mono-hull or Barge	Production	Storage, well proven, large deck space, deep water.	Sensitive to motions
Semi-submersible	Drilling, production	Low heave motion, well proven.	No storage.
Tension Leg Platform	Drilling, production	Roll, pitch and heave negligible, several varieties	No storage, sensitive to changes in payload
Spar	Drilling, production, storage (limited)	Easy shape.	Roll, pitch, and heave significant

Table 2. Categories of floating offshore structures – their uses, advantages and disadvantages

Source: http://www.eolss.net/sample-chapters/c05/e6-177-od-01.pdf

Additionally; the compulsory mooring system has also to be named. All these floating structures are subjected to the seabed by its mooring lines. They can be wire ropes, fibre ropes or chains meshed up in its infinity of possibilities.

To conclude with this little introduction to the offshore wind energy production; remark that in this project just the Tension Leg Platform (TLP) and the Spar-Buoy floating platforms are the ones to be studied and analysed.

Chapter 2. Numerical models creation and validation.

The main goal of this chapter is to create and validate, by the SeaFEM program, the numerical models for the two studied platforms in order to ensure that the results obtained are accurate enough. Firstly, it proceeds with an overview through the General Data and the Time Data established for this analysis which will be a common fact between the two structures modelled. Then a brief introduction to the NREL offshore 5MW baseline wind turbine is presented and finally the whole structure validation is described.

2.1. General properties

2.1.1. General Data

For both two cases the **General data** (see Figure 5) consists of, first of all, setting the water density to 1025kg/m^3.

Just waves are chosen in the Problem set up in order to study the waves effects on the floating platforms.

The analysis type is Seakeeping even though being both platforms fixed to the bottom (no seakeeping analysis would be necessary) in order to allow the body condition to be assigned to the geometrical entities representing the floating platforms.

To enlighten the calculus time and to allow the Traditional Postprocess to be used, the results files are set to be written in Binary 1.

Finally; apart from all the General and Loads results, the Kinematics: Movements, velocities, accelerations and Raos are established to be calculated.

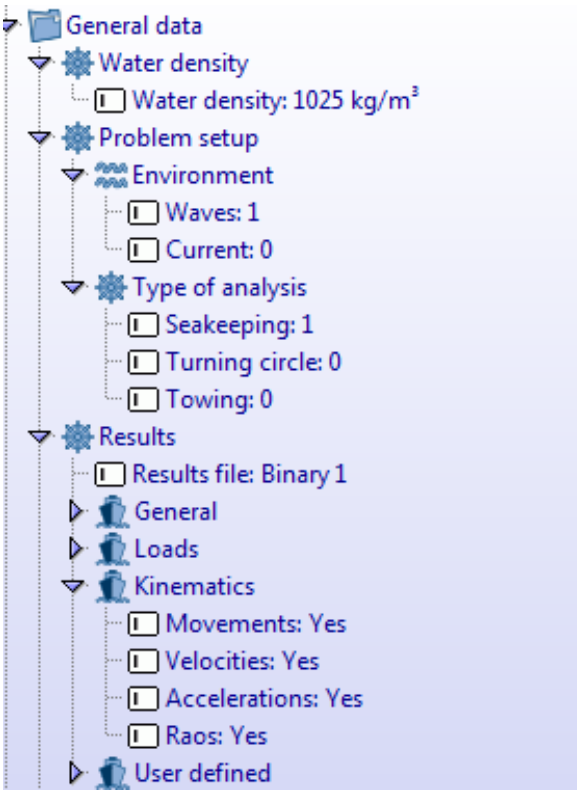

Figure 5. General data

2.1.2. Time data

On the other side; time data is also set (see Figure 6) equally to the two studied platforms: simulation time= 10000sec and start time recording= 1500sec.

The parameters established for the simulation time and the step time are just introduced to the program for the sake of guidance. SeaFEM internally evaluates the optimal values for both them according to Fourier analysis requirements resulting, for this analisys, a total simulation time of 1637.65sec and a time step of 0.268842sec.

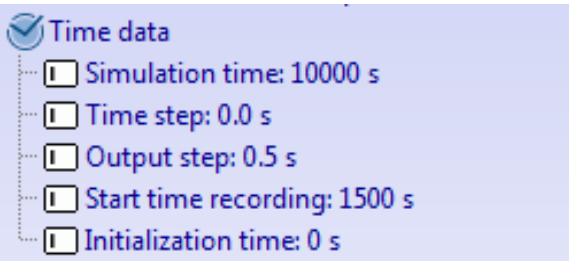

Figure 6. Time data

2.2. The NREL offshore 5MW baseline wind turbine

The NREL offshore 5MW baseline wind turbine (see Figure 7) used in this project was created to support theoretical studies targeted to asses offshore wind technology by the National Renewable Energy Laboratory (NREL). The baseline wind turbine was produced to become a representative utility-scale multi-megawatt turbine following the basic sizes and power ratings of the offshore wind turbines.

It consists of a conventional three-bladed upwind variable-speed variable blade-pitch-to feather-controlled turbine. It was created based on much broad design information from the published documents of turbine manufacturers like information on the Multibrid M50000 and RE power 5M prototype wind turbines as well as some publicly available properties from the conceptual models used in the WindPACT, RECOFF, and DOWEC projects.

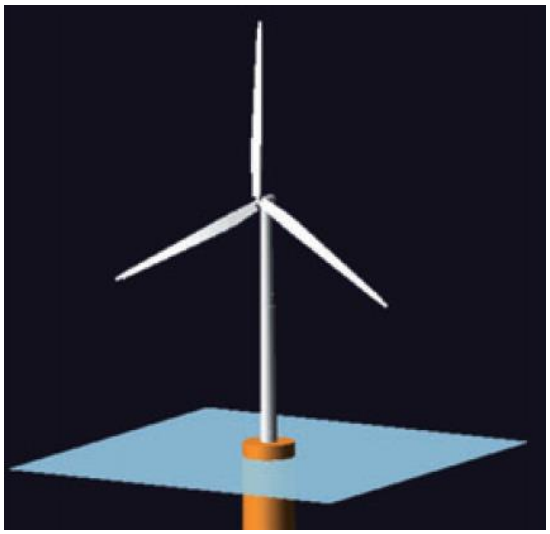

Figure 7. Wind turbine

Source: http://www.nrel.gov/docs/fy08osti/41958.pdf

Its' most significant properties (see Table 3) and it's mass, damping and stiffness matrices [4] are presented below. To find more information about the NREL offshore 5MW baseline wind turbine - including the aerodynamic, structural, and control-system properties—and the rationale behind its development see: http://www.nrel.gov/wind/pdfs/38060.pdf.

General			Wind Speed		
Rated power	5	**MW**	**Cut-in**	3	m/s
Rotor orientation		Upwind	**Rated power**	11,4	m/s
Rotor configuration	3	blades	**Cut-out**	25	m/s
	61,5	m length	**Cut-in rotor speed**	6,9	rpm
Rotor diameter	126	m	**rated rotor speed**	12,1	rpm
Hub diameter	3	m	**Overhung**	5	m
Hub height	90	m	**Weights**		
CM location			**Rotor mass**	110000	kg
x	-0,2	m	**Nacelle**	240000	kg
y	0	m	**Tower mass**	347460	kg
z	64	m	**Total mass**	697460	kg

Table 3. Wind turbine properties

Wind Turbine Mass Matrix:
Reference system: 0.0 0.0 0.0

0.7E+06	0	0	0	4.43E+07	0
0	0.7E+06	0	-4.43E+07	0	6.6E+06
0	0	0.7E+06	0	-6.6E+06	0
0	-4.43E+07	0	3.49E+09	0	0
4.43E+07	0	-6.60E+06	0	3.56E+09	0
0	6.60E+06	0	-5.13E+08	0	1.01E+08

Wind Turbine Damping Matrix:
Reference system: 0.0 0.0 0.0

4E+04	0	-1E+04	-2.5E+05	4E+06	8E+04
0	0	0	-1.1E+05	-1.8E+05	-5E+04
-1E+04	0	0	-4E+04	-9.2E+05	-3.3E+05
2.7E+05	-1E+05	0	1.62E+07	5.03E+07	1.38E+06
3.42E+06	6E+04	-1E+06	-2.39E+07	4E+08	5.90E+07
5E+04	-2E+04	2.2E+05	1.11E+07	5.26E+08	1.01E+08

Wind Turbine Stiffness Matrix:

Reference system: 0.0 0.0 0.0

0	0	0	0.3E+06	0.2E+06	0
0	0	0	-0.1E+06	0.3E+06	-0.07E+06
0	0	0	-0.3E+06	-0.4E+06	0
0	0	0	8.5E+06	-22.4E+06	59.7E+06
0	0	0	26.8E+06	28.9E+06	-4.1E+06
0	0	0	-1.2E+06	1.1E+06	-4.8E+06

2.3. The floating Tension Leg Platform (TLP) modelling and RAOs analyses

Tension Leg Platforms (see Figure 8) are floating platforms characterized by its mooring system, which keeps them in place, formed by cable-lines.

This kind of offshore platform has the particularity that the platform's buoyancy overcomes the weight of the platform. For this reason; it requires clusters of tight tendons, or what gives it its name, tension legs secured into the seabed. That tendons system is highly tensioned as a result of the platform hull buoyancy excess [5].

The tension leg mooring system allows horizontal movement with wave disturbances, but does not permit or dampens vertical motions, which makes TLPs a popular choice for stability [6].

Figure 8. TLP structure

Source: http://www.compositesworld.com/articles/wind-over-deep-water

2.3.1. Problem description

In the Problem description section many parameters related to the bathymetry depth and wave absorption have to be fixed (see Figure 9).

The bathymetry is set to 200m constant depth as specified in the D. Matha thesis [7].

The closest zone to the body is to be the study zone. This area is known as beach and there no artificial dissipation is introduced. Apart from that area, to avoid wave's superposition effects, wave absorption has to be activated. With this goal, a diameter around the studied body at 75m is set to delimitate the absorption area in which wave absorption is induced numerically to stabilize the results (see Figure 10).

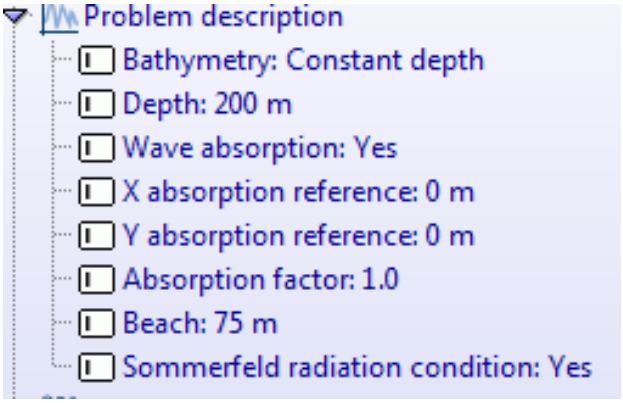

Figure 9. Environment data

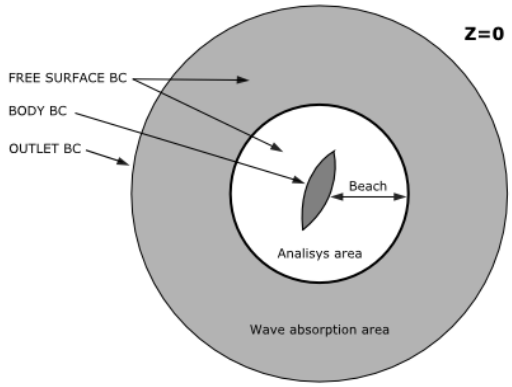

Figure 10. Beach and absorption area definition Source: SeakeepingFEM tutorial

2.3.2. Environment data

In this case, the environment data consists of an only wave spectrum (without considering any currents settings). The wave chosen is a White noise type which introduces a number of waves with frequencies uniformly distributed across an interval, and with the same amplitude direction. In the present cases (both TLP and Self-Buoy) the white noise spectra is used since we are mainly interested in the RAOs behaviour of the platforms.

This case features are (see Figure 11): 1m amplitude, 3 seconds shortest period, 20 seconds the longest and finally 40 wave's periods.

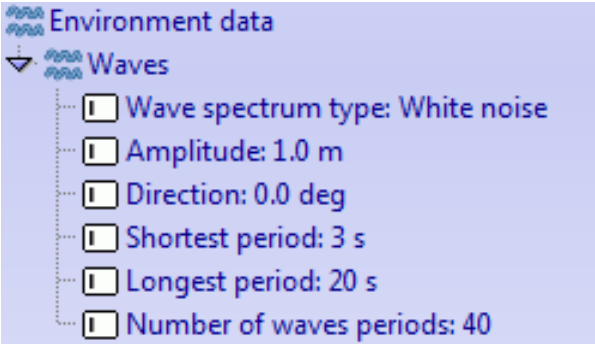

Figure 11. Environment data

2.3.3. Geometry and properties

As said in the abstract; the TLP used in this study is the one from the D. Matha thesis which's geometry (see Figure 12 - units in meters) and properties (see Table 4) are synthesized above.

Notice that the geometry created is a simplified model from the real TLP which just considers the cylindrical part of the TLP.

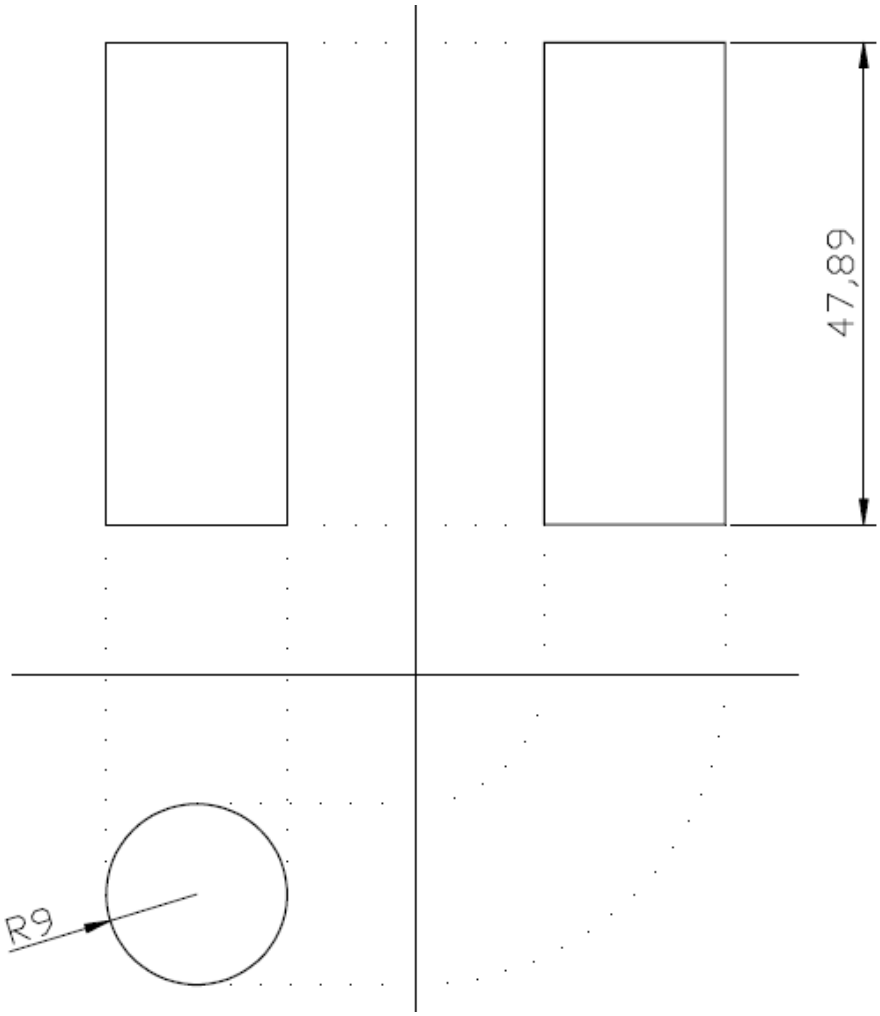

Figure 12. TLP geometry

General		Inertia:	
Total Draft	47.89 m	**Roll about CM**	453.7 $kg \cdot m^2$
Top Elevation	12.6 m	**Pitch about CM**	453.7 $kg \cdot m^2$
Platform diameter	18 m	**Yaw**	362.4 $kg \cdot m^2$
Weights		**CM location**	
Total mass	8654734 kg	**x**	0 m
		y	0 m
		z	-40.6 m

Table 4. Tension Leg Platform properties

Moreover; many other properties are necessary to be introduced to the numerical model being created like the TLP mass matrice, the mass, damping and stiffness wind turbine matrices and finally the stiffness mooring matrix. With this purpose the following TLC script is attached to the program:

```
proc TdynTcl_InitiateProblem { } {
TdynTcl_Add_Mass_Matrix 1 [list 0.0 0.0 0.0] [list \
          8.6E+06    0          0           0          -3.5+08     0 \
          0          8.6E+06    0          3.5+08      0          0 \
          0          0          8.6E+06    0           0           0 \
          0          3.5+08     0          1.5E+09     0          0 \
           -3.5+08   0          0          0           1.5E+10    0 \
          0          0          0          0           0          3.6E+08 ]
TdynTcl_Add_Mass_Matrix 1 [list 0.0 0.0 0.0] [list \
          0.7E+06    0          0          0           4.4E+07    0 \
          0          0.7E+06    0          -4.4E+07    0          6.6E+06 \
          0          0          7.0E+05    0           -6.6E+06   0 \
          0          -4.4E+07   0          3.5E+09     0          0 \
          4.4E+07    0          -6.6E+06   0           3.6E+09    0 \
          0          6.6E+06    0          -5.13E+08   0          1.0E+08 ]
TdynTcl_Add_Damping_Matrix 1 [list 0.0 0.0 0.0] [list \
          4E+04      0          -1E+04     -2.5E+05    4E+06      8E+04 \
          0          0          0          -1.1E+05    -1.8E+05   -5E+04 \
          -1E+04     0          0          -4E+04      -9.2E+05   -3.3E+05 \
          2.7E+05    -1E+05     0          1.6E+07     5.0E+07    1.4E+06 \
          3.4E+06    6E+04      -1E+06     -2.4E+07    4E+08      5.9E+07 \
          5E+04      -2E+04     2.2E+05    1.1E+07     5.3E+08    1.0E+08]
```

```
TdynTcl_Add_Stiffness_Matrix 1 [list 0.0 0.0 0.0] [list \
          0          0          0          3.0E+05    2.0E+05    0 \
          0          0          0          -1.0E+05   3.0E+05    -7.0E+04 \
          0          0          0          -3.0E+05   -4.0E+05   0 \
          0          0          0          8.5E+06    -2.2E+07   6.0E+07 \
          0          0          0          2.7E+07    2.9E+07    -4.1E+06 \
          0          0          0          -1.2E+06   1.1E+06    -4.8E+06 ]
TdynTcl_Add_Stiffness_Matrix 1 [list 0.0 0.0 0.0] [list \
          2.5E+05    0          1.5E+06    0          -7.3E+06   0 \
          0          2.1E+05    0          6.3E+06    0          -5.1E+05 \
          1.5E+06    0          7.0E+07    0          -4.5E+07   0 \
          0          6.2E+06    0          1.5E+10    0          -4.1E+08 \
          -6.9E+06   0          -3.2E+07   0          1.5E+10    0 \
          0          0          0          -3.5E+08   0          9.5E+07 ]
TdynTcl_Message "TdynTcl_DefineBodyData finished!!!" notice
}
```

2.3.4. Model creation

Once introduced some of the calculus parameters to the program; the body and whole geometry is created. First of all, to enable a better control of the entities which will be drawn; some different layers are created (see Figure 13).

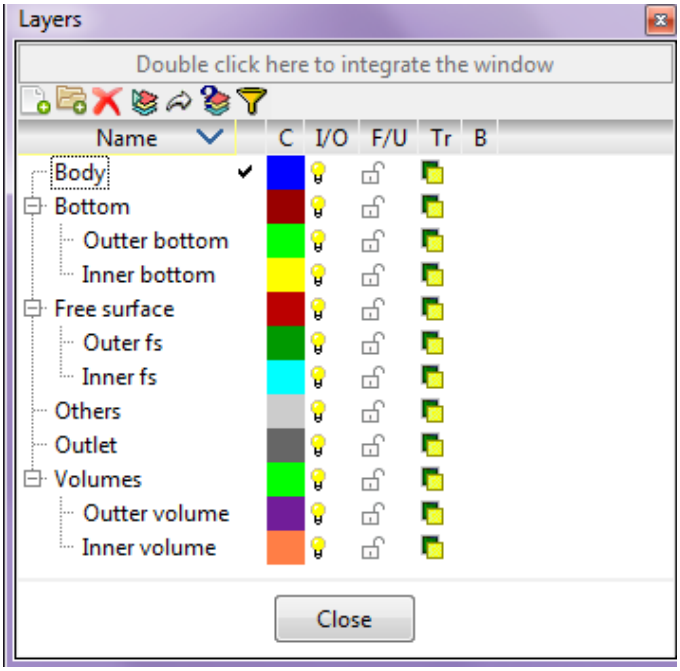

Figure 13. TLP Layers created

Then the body is built, followed by the inner water volume and finishing with an outer water volume (see Figure 14). Those volumes are created to guarantee precision when calculating and also to avoid over-calculus as being this an easy way to keep a closer control to the mesh elements sizes which will be

defined afterwards. Sometimes these cylindrical bodies are established to be the division between the wave absorption area and the non-absorption one. Nevertheless here is not the cause and its diameters are: 50m the inner volume and 600m the outer volume and both depths are 200m.

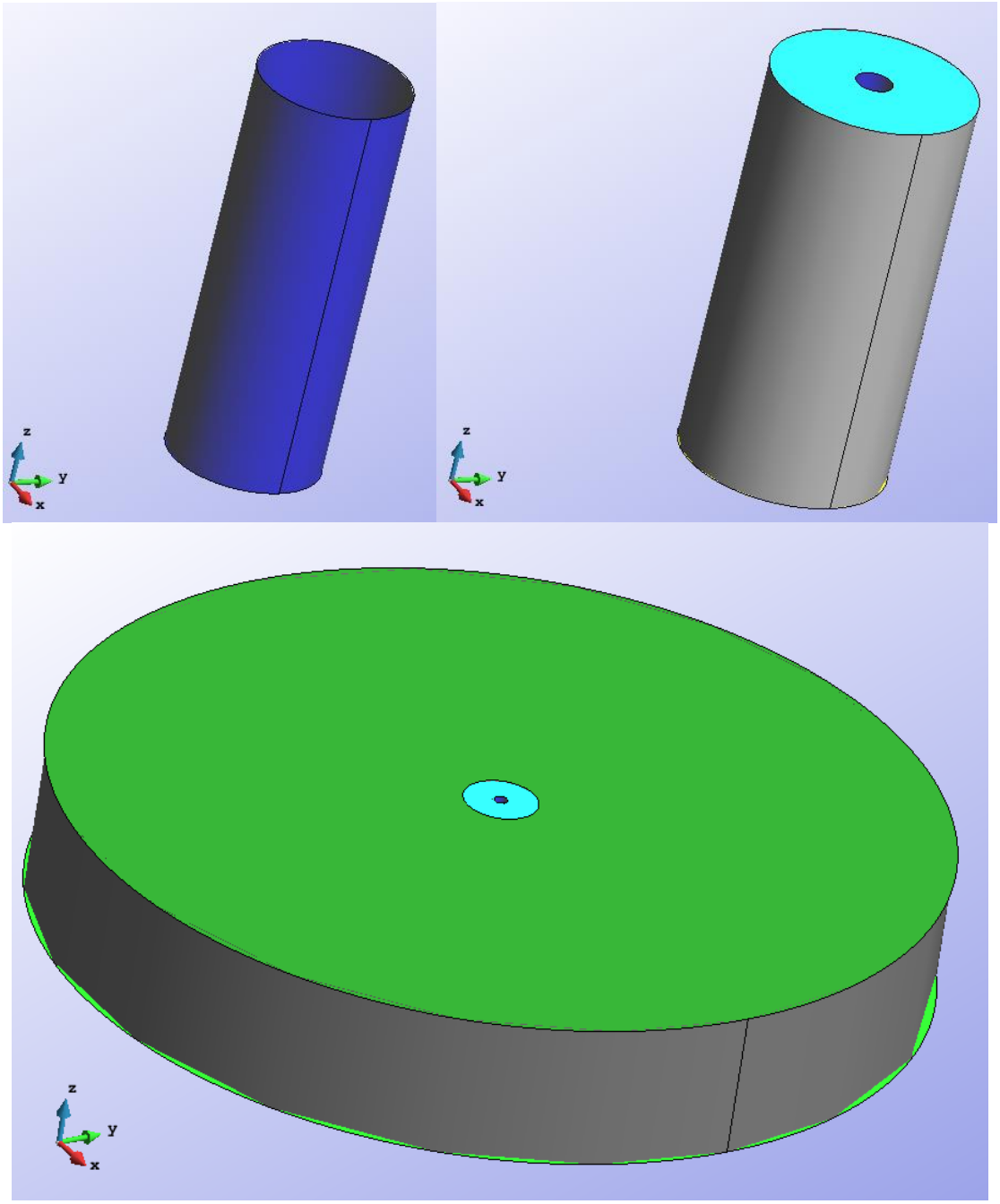

Figure 14. TLP creation steps

2.3.5. Body data

Body data parameters have to be set to the studied geometry (see Figure 15).

Being known the whole inertia radius parameters, they are introduced to the program as a matrix in the Body properties.

Surge, heave and pitch are established as degrees of freedom, which means that sway, roll and yaw are fixed.

In order to obtain rational heave results, the external force Z is set as a function: "Mass*g-vol*density*g", which just emphasizes that there must be equilibrium between the weight and the buoyancy forces.

Initial position and velocity are fixed as 0 in all directions.

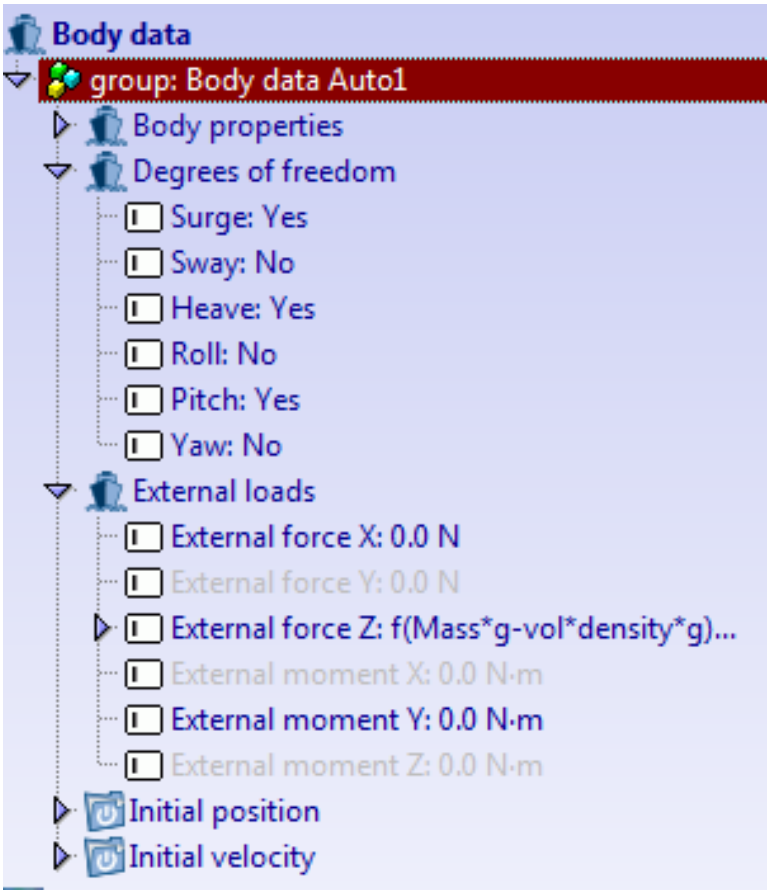

Figure 15. Body data

2.3.6. Boundary conditions

Having all the previous data set, just the boundary conditions have to be assigned to the geometry created to fulfil the numerical problem.

This case just needs two boundary conditions (see Figure 16):

- the **free surface boundary condition** applied to all the geometry surface entities located at the free surface of the model, in this case to the surfaces situated at z=0m.
- And the **outlet boundary condition** assigned to the outmost boundary of the computational domain, in this case to the external surface of the external cylinder.

Figure 16. Boundary conditions

2.3.7. Mesh creation

Being Tdyn a program which calculates with Finite Elements Method; a mesh needs to be created and a mesh optimization process needs to be completed. Different and concrete initial mesh size is set (see Table 5 and see Figure 17). And a maximum elements size of 50 with an unstructured size transitions of 0.3.

Size	Points	Lines	Surfaces	Volumes
1	– Body – Inner free surface	– Body – Inner free surface	– Body – Inner free surface	
5		– Inner's cylinder vertical part	– Inner's cylinder vertical part	– Inner volume
10	– Bottom	– Bottom	– Bottom	

Table 5. Initial mesh elements size set.

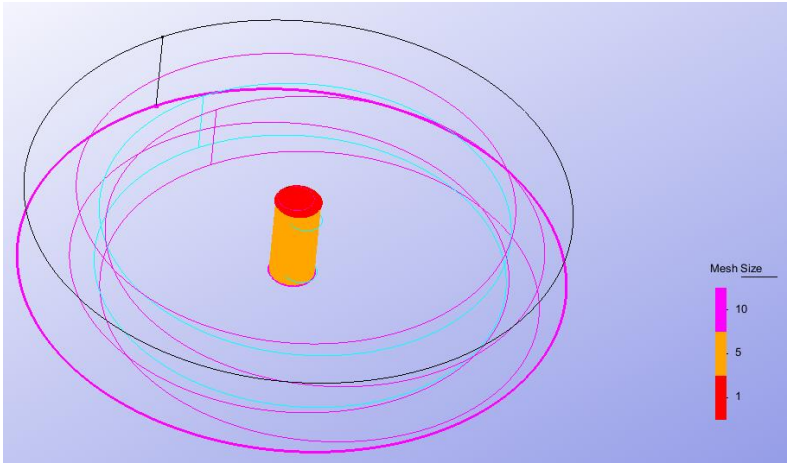

Figure 17. TLP Mesh initial asigned sizes

By this point the initial mesh is used to obtain the first RAO results. And once they are considered as correct results, the mesh optimization is done.

2.3.8. RAO results

After a long calculus time, between 14 and 15 hours, the first RAO pitch results are obtained (see Figure 18). Then these results have to be compared with ones from a reliable source which in this case are the results from the same TLP found in the SeaFEM tutorial (see Figure 19) [8].

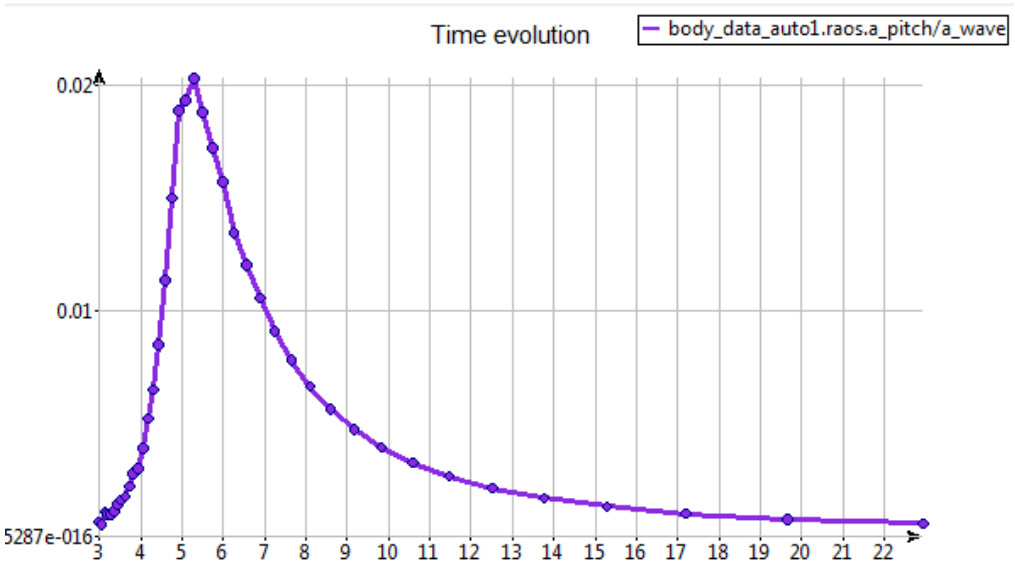

Figure 18. Obtained TLP pitch RAO results

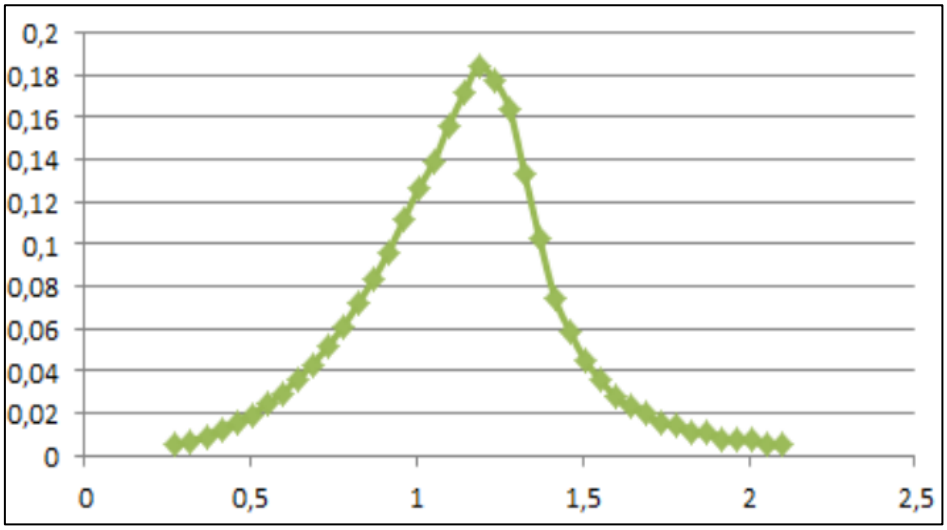

Figure 19. SeaFEM TLP pitch RAO results (vertical axis [m] and horitzontal axis [rad/s])

At first sight those two results graphs don't seem to look like the same, but this is just because they are not in the same units. In order to adapt the obtained results to the ones found in the tutorial, the pitch RAO results have been multiplied by its radius of gyration (9m) and the frequencies have been converted from sec to rad/sec . And then in the vertical axis the displacements at the end of the TLP structure are obtained (see Figure 20).

And definitively this last graph actually looks like the one from the results. So we can conclude that the TLP geometry was greatly created and it must be observed that the TLP natural frequency is about 1.1868 rad/s.

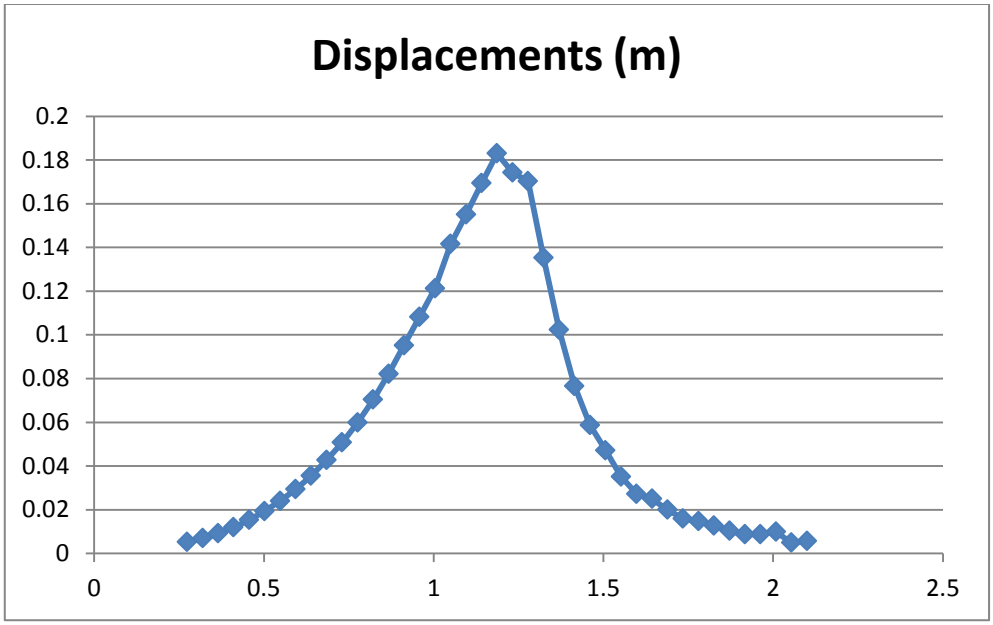

Figure 20. TLP obtained displacements

2.3.9. Mesh optimization

Once all the results are checked, the optimization mesh procedure needs to be done in order to reduce the calculus time.

To proceed with the mesh optimization; the structure pitch RAO is calculated using many different meshes. Once done it, we will find out which are the meshing effects to the RAO results by only using different mesh sizes (see Figure 21), comparing them, and finding which is the most precise and lasts less when calculating.

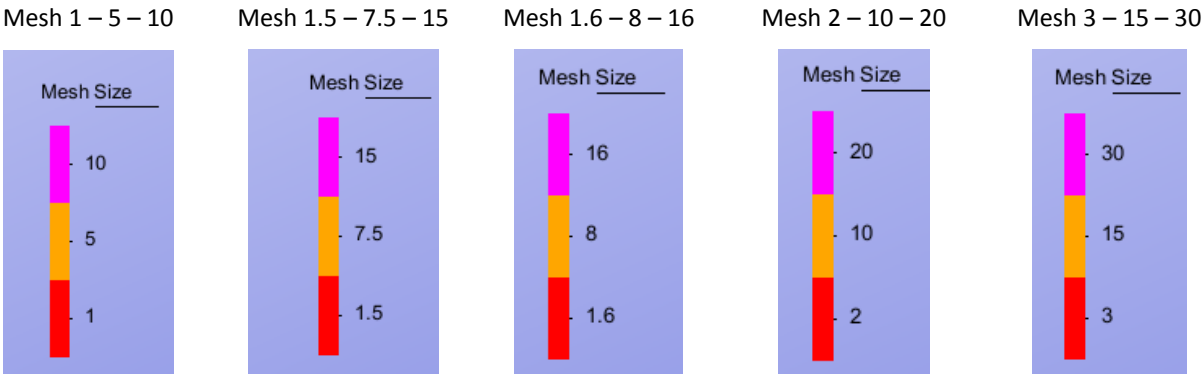

Figure 21. Different mesh sizes considered

Then the RAO accuracy is studied. Firstly, we are comparing the natural frequency of the structure; how the different amount of nodes (and elements) affects to the result. In order to do that, a graph gathering all the different results obtained on each mesh is presented (see Figure 22).

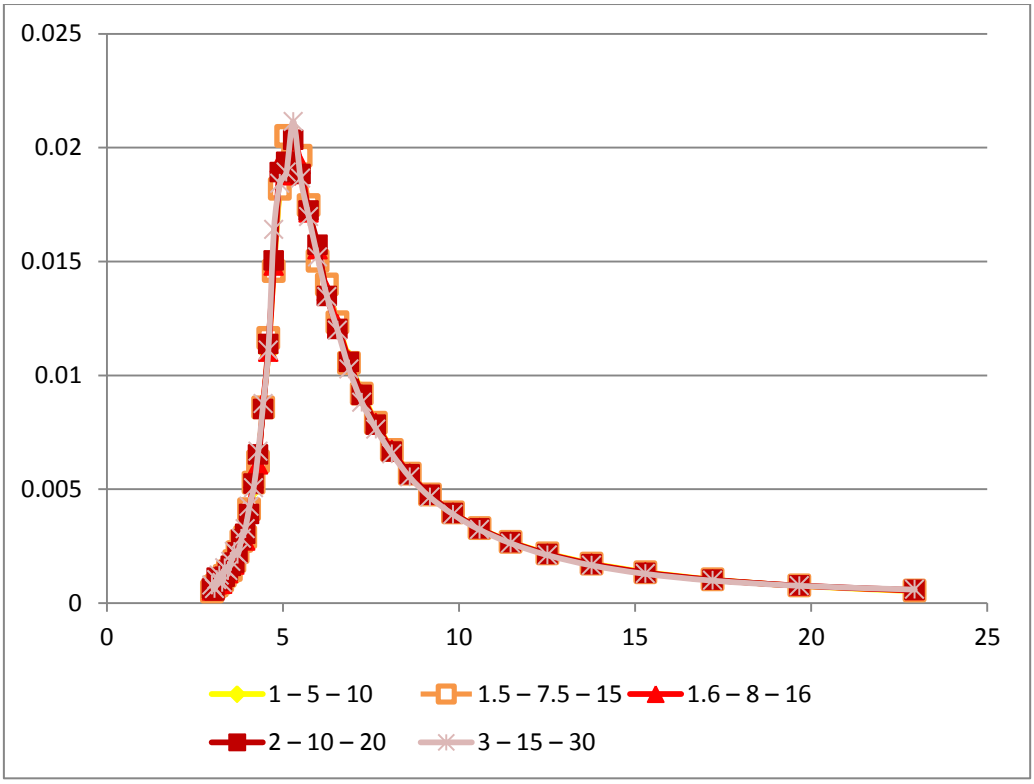

Figure 22. Different RAO results obtained acording to the mesh used

To conclude, what we find out is that even though increasing the mesh 3 times the original established, accurate - and even closest to the compared to ones- results are obtained being the structure natural frequency of 5.294s (1.1869 rad/sec) instead of the original 5.098 sec (1.232 rad/sec) obtained with the first mesh.

On the other side, one of the also important facts to consider when optimizing a mesh is how the mesh size affects to the computational time. Through all these calculations (see Table 6), the time has decreased considerably decreased from 14.30 hours to just 47 minutes.

Mesh name	Computational time
1 – 5 – 10	52194.2sec= 14h 29min 54.2sec
1.5 – 7.5 – 15	21880.2sec = 6h 4min 40.2sec
1.6 – 8 – 16	17694.1sec= 4h 54min 54.1sec
2 – 10 – 20	16125.6sec = 4h 28min 45.6sec
3 – 15 – 30	2804.3sec = 46 min 44.3sec

Table 6. TLP mesh optimizing computational time

To end up with the mesh optimizing, as having positive aspects for both RAO accuracy and Computational time reduction, the final mesh set is the one of its minimum elements size assigned of 3m (see Table 7).

Size	Points	Lines	Surfaces	Volumes
3	– Body – Inner free surface	– Body – Inner free surface	– Body – Inner free surface	
15		– Inner's cylinder vertical part	– Inner's cylinder vertical part	– Inner volume
30	– Bottom	– Bottom	– Bottom	

Table 7. TLP final elements size assigned

Once the mesh optimization is done these are the final elements sizes obtained and the definitive meshes (see Figure 23).

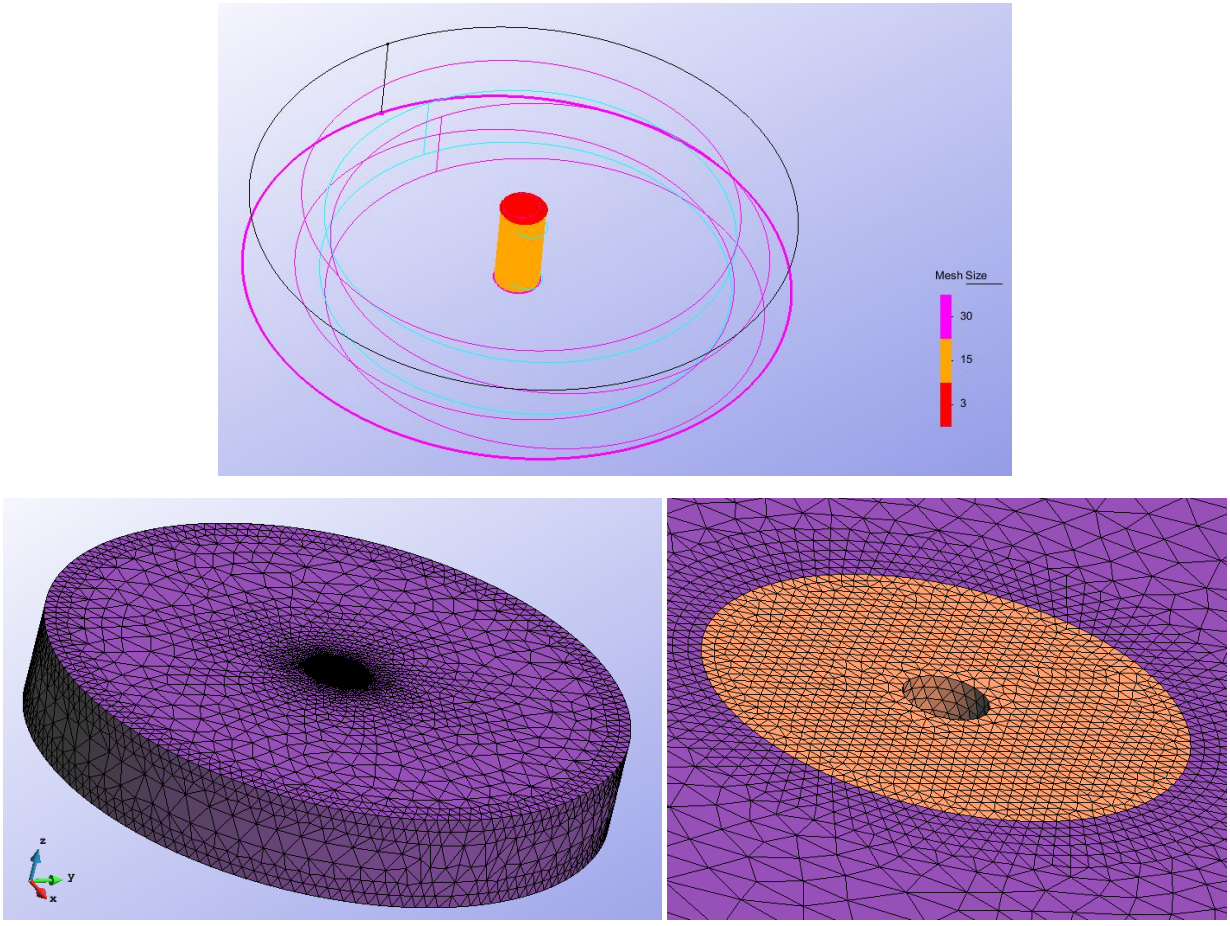

Figure 23. TLP final mesh

2.4. The floating Spar-Buoy modelling and RAOs analyses

The OC3 - Hywind Spar-Buoy consists of two cylindrical sections connected by a linear tapered conical region. Being designed for deep waters of up to 320 meters, the Spar-Buoy integrates an elongated cylindrical tank with a high aspect ratio (see Figure 24).

In order to improve the geometry stability; at the bottom tank, ballast is included. This helps decrease the center of gravity of the cylinder and so it becomes more stable.

Furthermore, the Spar-Buoy can be moored to the ocean bed with either taut or catenary lines to afford extra stability [9].

This eye-catching simplicity of the slender cylinder model has also its weak points resulting from this geometry and mooring properties a source of extra fatigue loads to the whole structure [10].

Figure 24. Spar-buoy platform

Source: http://www.compositesworld.com/articles/wind-over-deep-water

2.4.1. Problem description

As well as in the TLP floating structure, Problem description has also a beach area of 75m and almost all wave absorption parameters equals to the ones set previously in the TLP but the depth (see Figure 25).

The Spar Buoy studied in this project is a floating platform calculated for a 320m depth.

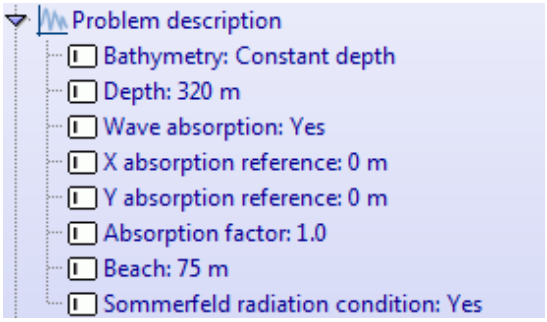

Figure 25. Problem description

2.4.2. Environment data

The Environment data consists of an only wave environment – no currents set – (see Figure 26). A White noise spectrum of 1m amplitude, 25 seconds the shortest period and 67 seconds the longest and a number of wave periods of 40.

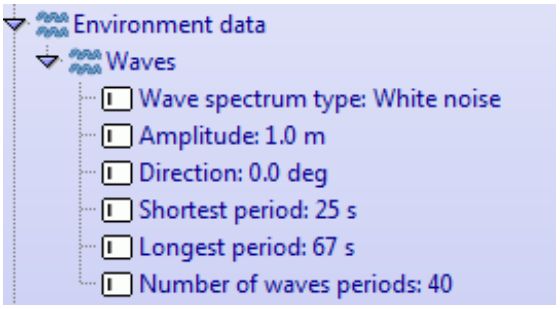

Figure 26. Environment data

Those shortest and longest wave periods are set this way in order to enable the afterwards RAO result comparison.

2.4.3. Geometry and properties

The Spar Buoy used in this project is the IEA Offshore Code Comparison Collaboration (OC3) –Phase IV Hywind Spar which's geometry below the sea water level (see Figure 27) and its properties (see Table 8) are synthesized beneath [12].

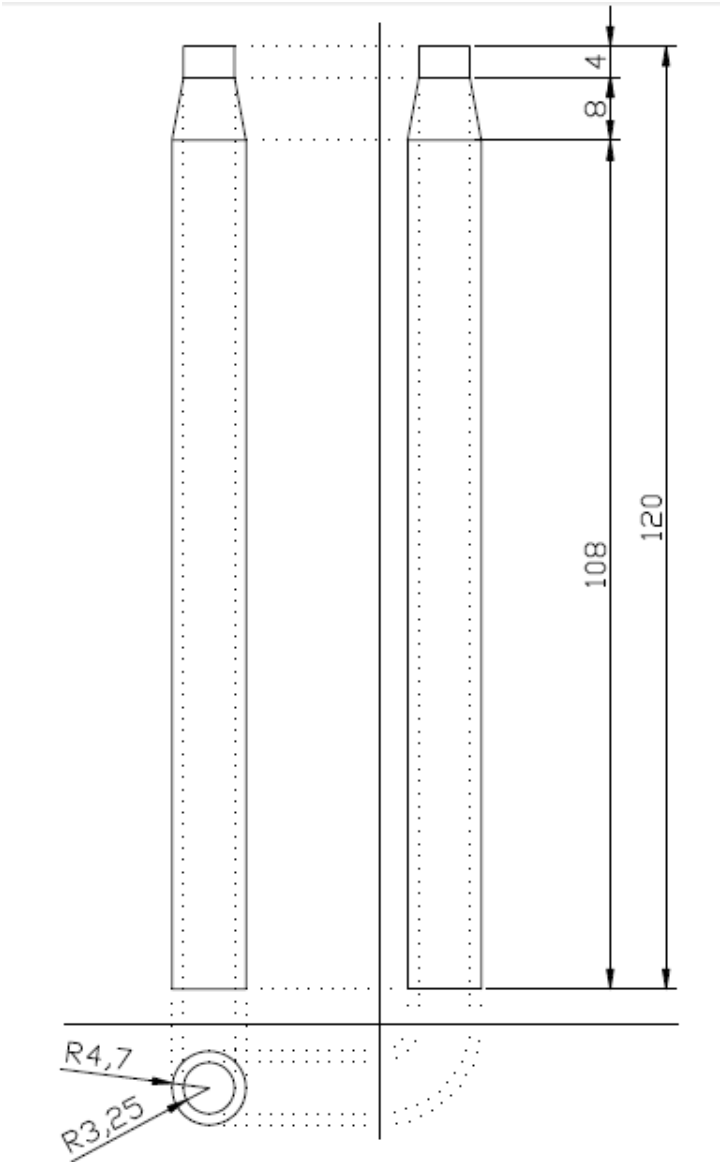

Figure 27. Spar Buoy geometry

General			Inertia:	
Total Draft	-120 m		**Roll about CM**	4,23E+09 kg·m^2
Top Elevation	10 m		**Pitch about CM**	4,23E+09 kg·m^2
Top of Taper	-4 m		**Yaw**	1,64E+08 kg·m^2
Bottom of Taper	-12 m		**CM location**	
∅ Top Taper	6,5 m		**x**	0 m
∅ Below taper	9,4 m		**y**	0 m
Weights			**z**	-89,9155 m
Total mass	7466330 kg			

Table 8. Floating Spar Buoy properties

As well as with the TLP; there are many other properties to be introduced like the platform mass, the wind turbine mass, damping and the stiffness matrices and finally the linearized mooring stiffness matrix. They are all included to the program by this TLC script:

```
proc TdynTcl_InitiateProblem { } {
TdynTcl_Add_Mass_Matrix 1 [list 0.0 0.0 -89.92] [list \
          7.5E+06    0          0          0          0          0 \
          0          7.5E+06    0          0          0          0 \
          0          0          7.5E+06    0          0          0 \
          0          0          0          4.2E+09    0          0 \
          0          0          0          0          4.2E+09    0 \
          0          0          0          0          0          1.6E+8 ]
TdynTcl_Add_Mass_Matrix 1 [list 0.0 0.0 0.0] [list \
          0.7E+06    0          0          0          4.4E+07    0 \
          0          0.7E+06    0          -4.4E+07   0          6.6E+06 \
          0          0          7.0E+05    0          -6.6E+06   0 \
          0          -4.4E+07   0          3.5E+09    0          0 \
          4.4E+07    0          -6.6E+06   0          3.6E+09    0 \
          0          6.6E+06    0          -5.13E+08  0          1.0E+08 ]
TdynTcl_Add_Damping_Matrix 1 [list 0.0 0.0 0.0] [list \
          4E+04      0          -1E+04     -2.5E+05   4E+06      8E+04 \
          0          0          0          -1.1E+05   -1.8E+05   -5E+04 \
          -1E+04     0          0          -4E+04     -9.2E+05   -3.3E+05 \
          2.7E+05    -1E+05     0          1.6E+07    5.0E+07    1.4E+06 \
          3.4E+06    6E+04      -1E+06     -2.4E+07   4E+08      5.9E+07 \
          5E+04      -2E+04     2.2E+05    1.1E+07    5.3E+08    1.0E+08]
TdynTcl_Add_Stiffness_Matrix 1 [list 0.0 0.0 0.0] [list \
          0          0          0          3.0E+05    2.0E+05    0 \
          0          0          0          -1.0E+05   3.0E+05    -7.0E+04 \
          0          0          0          -3.0E+05   -4.0E+05   0 \
          0          0          0          8.5E+06    -2.2E+07   6.0E+07 \
          0          0          0          2.7E+07    2.9E+07    -4.1E+06 \
          0          0          0          -1.2E+06   1.1E+06    -4.8E+06 ]
```

```
TdynTcl_Add_Stiffness_Matrix 1 [list 0.0 0.0 0.0] [list \
          4.1E+04    0          0          0          -2.8E+06   0 \
          0          4.1E+04    0          2.8E+06    0          0 \
          0          0          1.2E+04    0          0          0 \
          0          2.8E+06    0          3.1E+08    0          0 \
          -2.8E+06   0          0          0          3.1E+08    0 \
          0          0          0          0          0          1.2E+07 ]
TdynTcl_Message "TdynTcl_DefineBodyData finished!!!" notice
}
```

2.4.4. Model creation

The first step when creating a new geometry is the layers creation (see Figure 28). All entities are going to be organized among them to make it easier to work with or assigning properties to them.

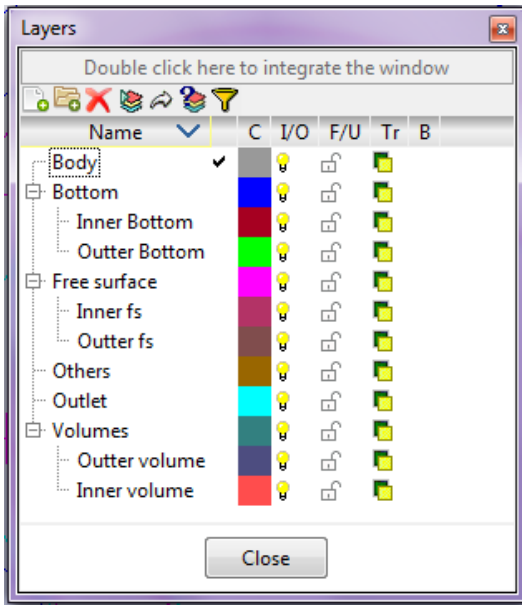

Figure 28. Spar-Buoy Layers created

The spar is shaped by drawing two cylinders and then matching them with a conical sector and its inner and outer volumes are drawn too (see Figure 29).

Also the two external volumes are created to get more mesh size precision. Its dimensions are, as well as in the TLP Model creation, of about 50m and 600m external diameters, and 200m depth. Again differing with the beach parameter set in the Problem description, although sometimes it is created so it coincides.

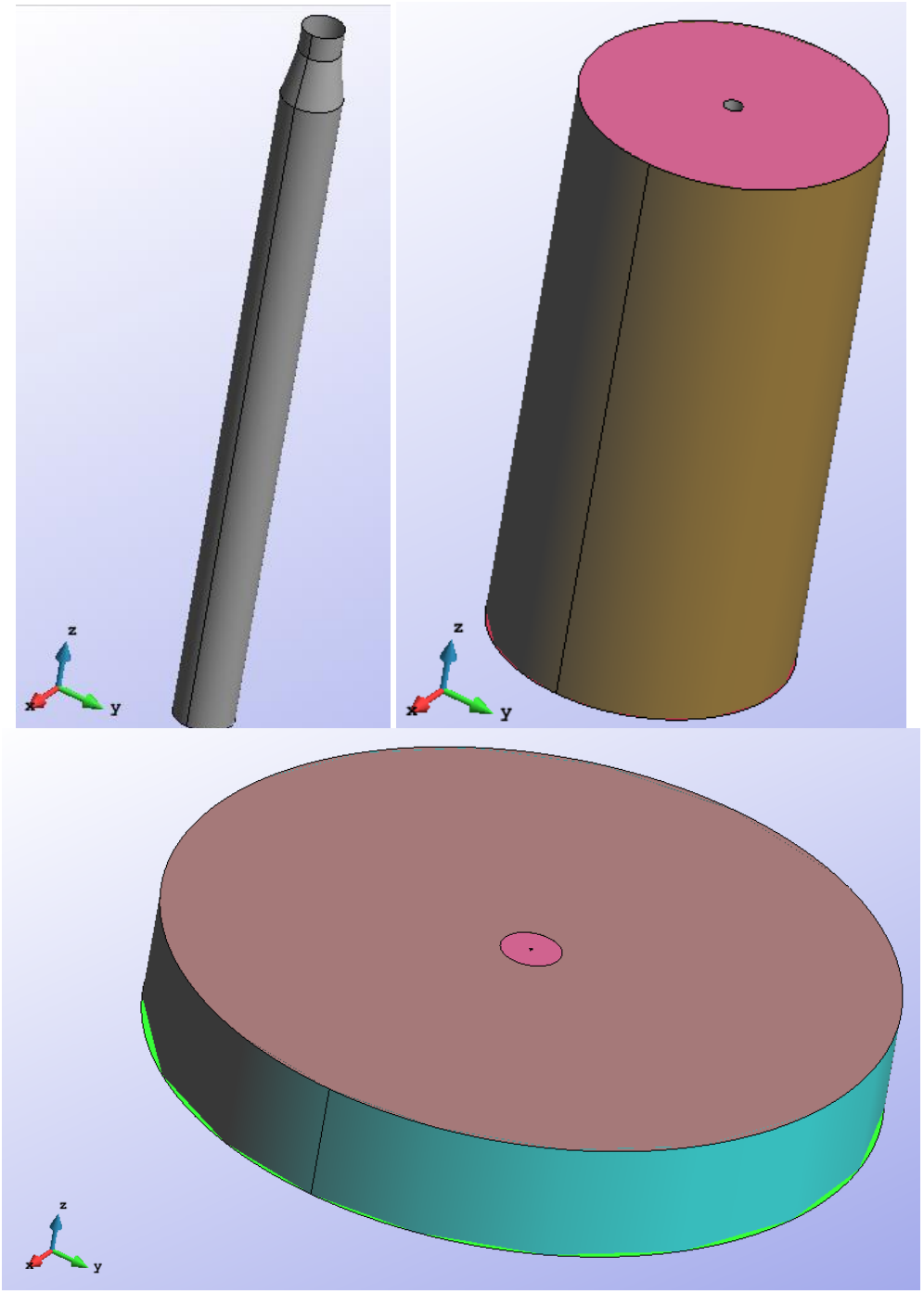

Figure 29. Floating Spar Buoy creation steps

2.4.5. Body data

Body data parameters are fixed to the spar buoy geometry (see Figure 30).

Not many individual body properties are set in this geometry but actually this really does not matter as they have been included to the numerical model by the TLC script.

Surge, heave and pitch are recognised as degrees of freedom and sway, roll and yaw are fixed.

In order to obtain rational heave results, the external force Z is set as a function: "Mass*g-vol*density*g", which just emphasizes that there must be equilibrium between the weight and the buoyancy forces.

Initial position and velocity are considered as 0 in all directions.

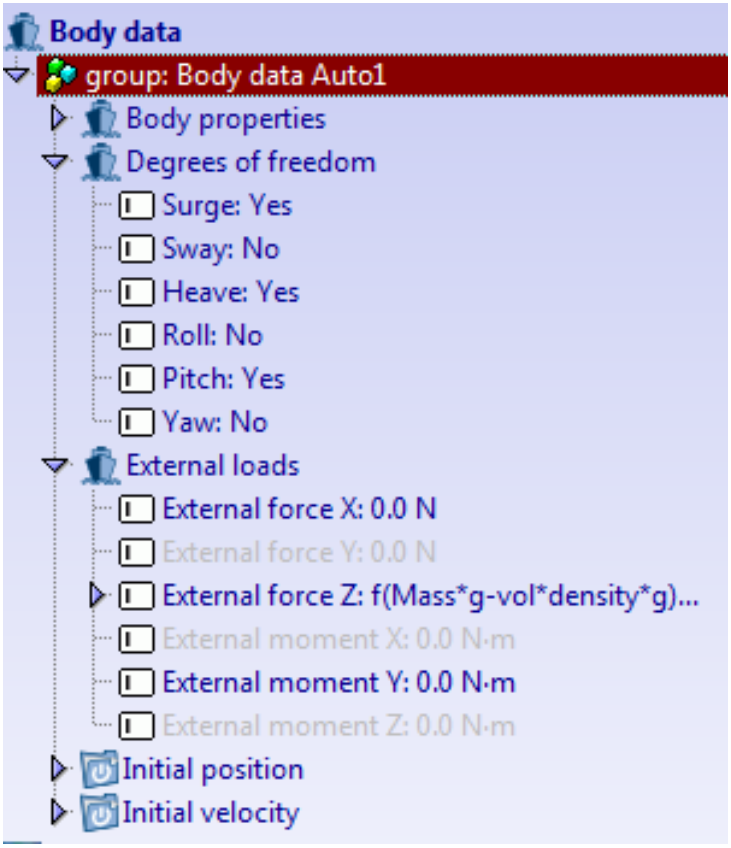

Figure 30. Body data

2.4.6. Boundary conditions

Once all the previous data is set, the assignation of the boundary conditions is the step to follow with again to fulfil the numerical problem **(see Figure 31)**.

This platform needs 3 boundary conditions:

- the **free surface boundary condition** applied to the surfaces situated at z=0m.
- The **outlet boundary condition** assigned to the external surface of the external cylinder.
- And finally the **bottom condition** is assigned to the surfaces located at the bottom of the whole geometry created in order to enable the program know that though the geometry bottom is there, the true bottom is far below what is drawn.

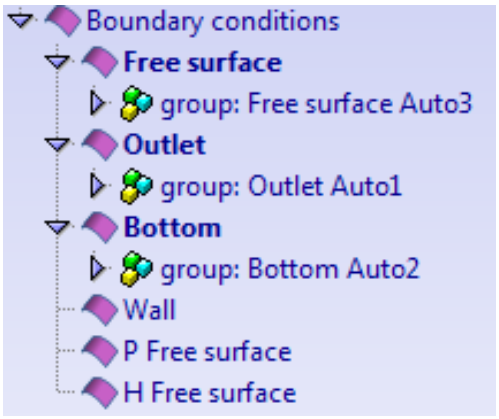

Figure 31. Boundary conditions

2.4.7. Mesh creation

The last step before seeing results is the mesh creation. At first time some orientated values are set to some elements (see Table 9 and see Figure 32) and later those values are going to be improved by a mesh optimization process. The maximum general elements size is set to 50 with an unstructured size transition of 0.3.

Size	Points	Lines	Surfaces	Volumes
2	– Body – Inner free surface	– Body – Inner free surface	– Body – Inner free surface	
10		– Inner's cylinder vertical part	– Inner's cylinder vertical part	– Inner volume
20	– Bottom	– Bottom	– Bottom	

Table 9. Initial mesh elements size set.

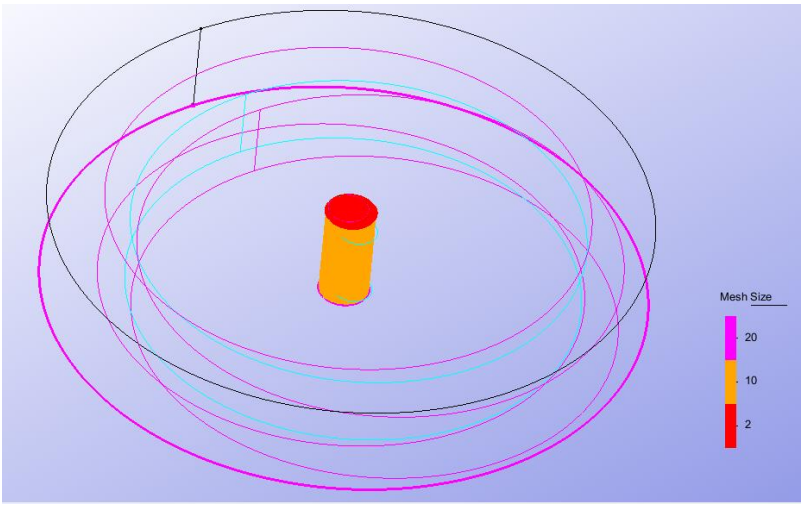

Figure 32. TLP Mesh initial asigned sizes

In order to get the very first RAO results, this mesh will work. If they are considered as correct results it will be proceeded with a mesh optimization process to reduce future calculus time.

2.4.8. RAO results

Once the whole numerical model is created, the calculus start and with the first mesh set the results are obtained. The first Heave RAO results are obtained approximately 25hours after calculation started (see Figure 33). This time the RAO parameter studied is the heave due to its notorious trajectory followed on the RAO heave results obtained in the Investigation of Response Amplitude Operators for Floating Offshore Wind Turbines by NREL[13] (see Figure 34).

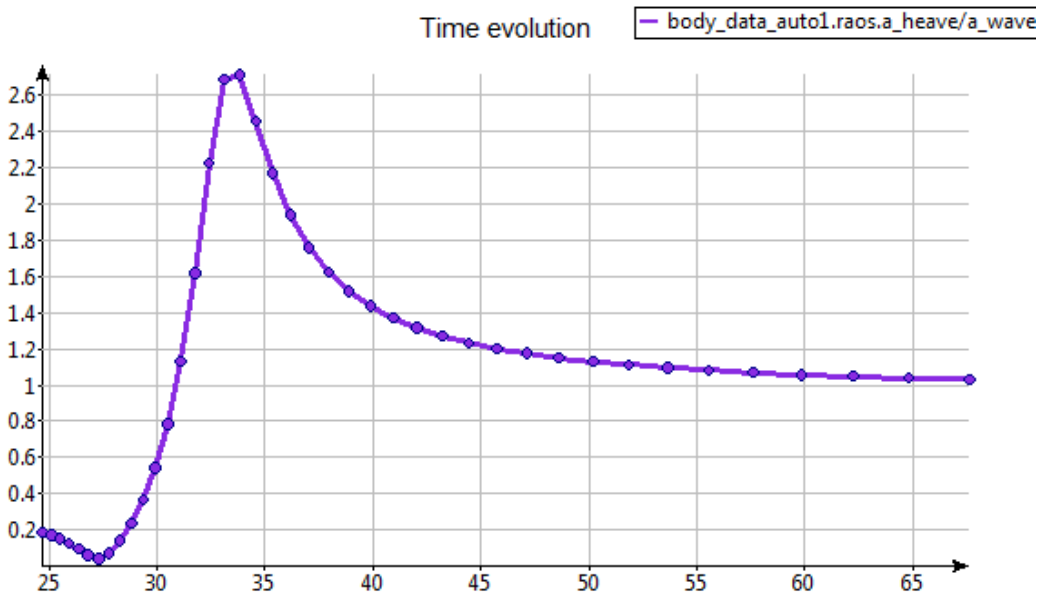

Figure 33. SeaFem Obtained Spar-Buoy heave RAO results (horizontal axis in seconds)

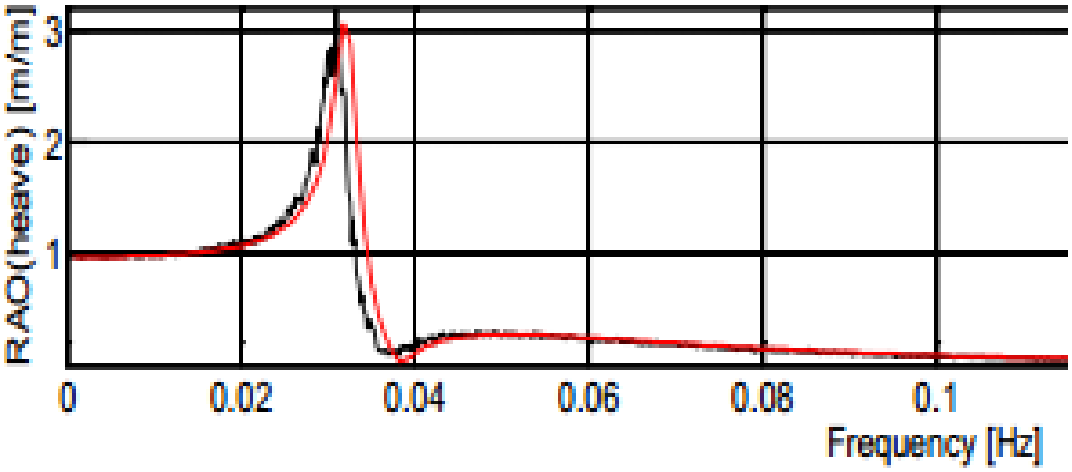

Figure 34. Spar-Buoy heave RAO results

To get a better look to the results, the horizontal axis has to be established in the same dimensions as in the NREL results obtained. This time it the inversion of the seconds values is necessary to convert them to Hz (see Figure 35).

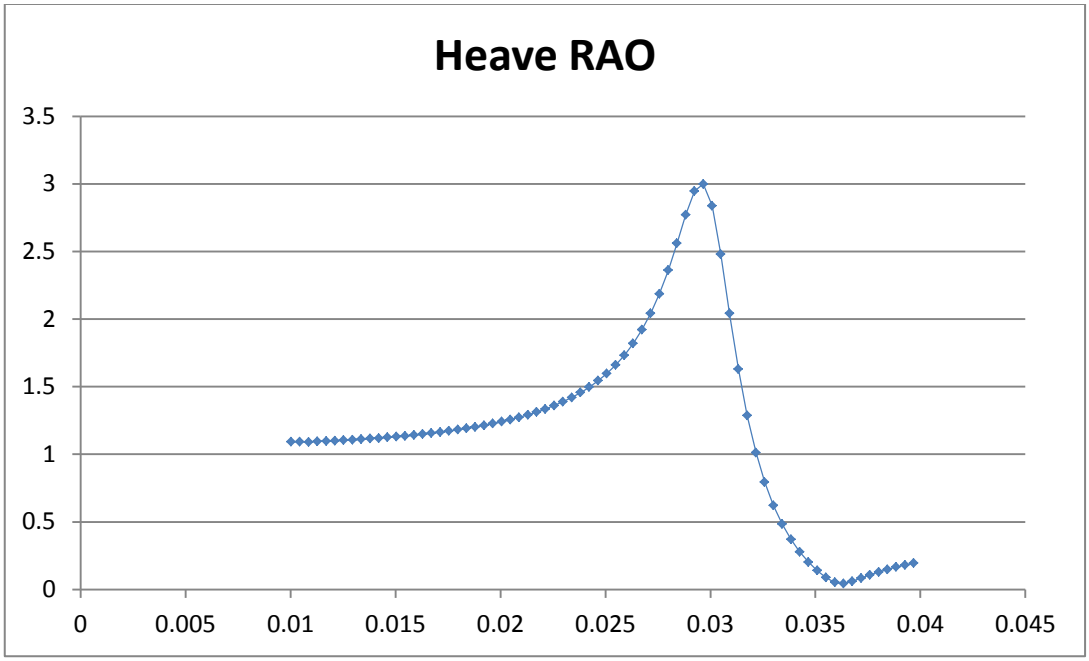

Figure 35. TLP obtained displacements

Finally, both graphs look much like the same. It can be concluded that the Spar-Buoy was properly created having its natural frequency around the 0.02966Hz (=33.71sec).

2.4.9. Mesh optimization

To go through the mesh optimization, the structure heave RAO must be calculated with different meshes (see Figure 36).

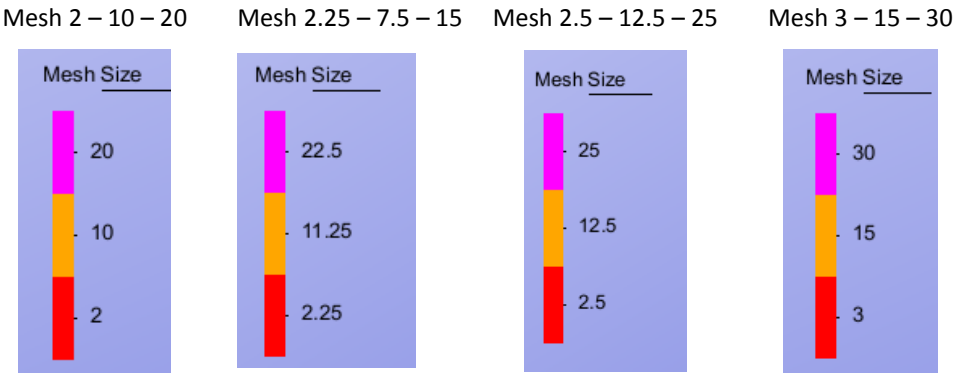

Figure 36. Different mesh sizes considered

The RAO accuracy study goes on by comparing different heave RAO results with the different mesh sizes considered. All the results obtained on each mesh are presented on the following graph (see Figure 37).

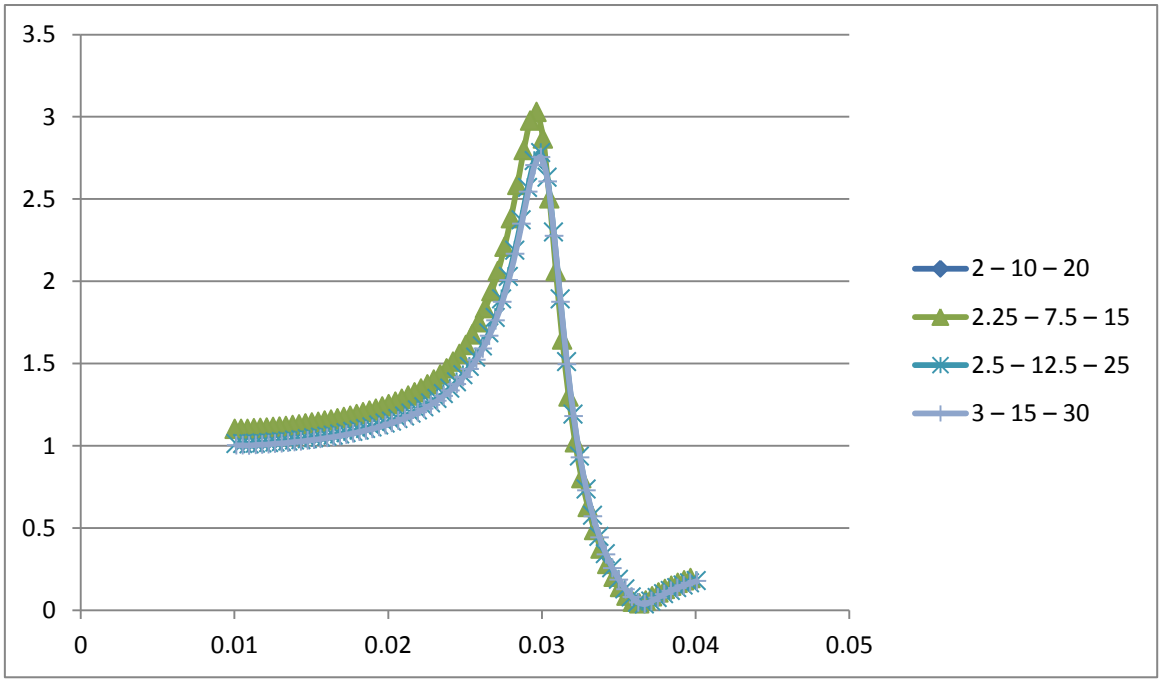

Figure 37. Different Spar-Buoy RAO results obtained acording to the mesh used

Finally from the first mesh to the last one it is found out that the structure natural frequencies obtained just vary from 0.02966Hz (33.71sec) in the first mesh to 0.029958Hz (33.40sec) in the last mesh.

As it is always known, computational time is an important parameter to be taken into account when doing a mesh optimization. In the following table results from all mesh computational time are shown (see Table 10), the computational time has decreased from the first 6 hours to just 87 minutes.

Mesh name	Computational time
2 – 10 – 20	22950.4sec = 6h 22min 30.4sec
2.25 – 7.5 – 15	9362.0sec= 2h 36min 2sec
2.5 – 12 – 25	6873.1sec = 1h 54min 33.1sec
3 – 15 – 30	5237.1sec = 1h 27min 17.1sec

Table 10. Spar-Buoy mesh optimizing computational time

Finally the mesh optimizing process can be concluded by selecting the mesh which gives us the most accuracy results with the least computational time, so the final mesh elements size is assigned to 3m size to the smallest elements (see Table 11). And the final mesh is created (see Figure 38).

Size	Points	Lines	Surfaces	Volumes
3	– Body – Inner free surface	– Body – Inner free surface	– Body – Inner free surface	
15		– Inner's cylinder vertical part	– Inner's cylinder vertical part	– Inner volume
30	– Bottom	– Bottom	– Bottom	

Table 11. TLP final elements size assigned

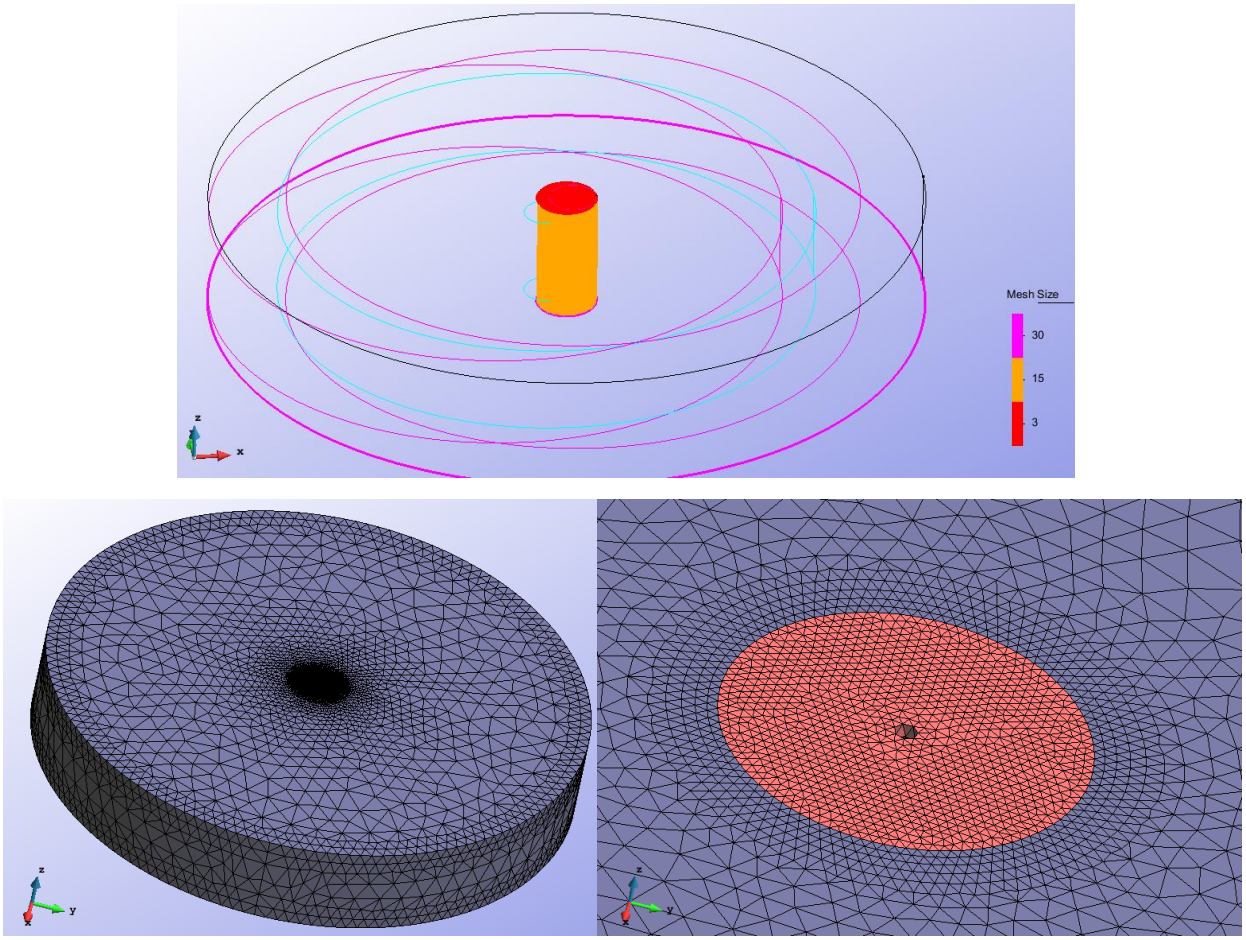

Figure 38. Floating Spar Buoy final mesh

Chapter 3. Mooring analysis

By the time, the RAOs calculation enabling cases have been created for both two structures. In this chapter two new twin new cases are created for each floating platform. One with the mooring stiffness matrix and the other with non-linear mooring lines created as explained forewards.

Once have been both twin cases created a motion results comparison is done. Why is this motion results comparison necessary?

> Stiffness matrices coefficients on the mooring lines contain the mooring properties referring just to the motions related with the displacements. It is useful when studying static motions of the floating structure but it loses accuracy when considerable motion is taken into account.
>
> To considerably improve the calculus results, and gain noticeably precision, non-lineal dynamic analysis, have to be fulfilled. Foremost, programs like SeaFEM have a really easy-programing procedure in which those mooring lines can be created contrasting with the actual difficulty.

And finally the last part of this Chapter 3 is dedicated to analyse the forces which the mooring lines induce to both floating platforms.

3.1. General properties

Like in the last chapter, the environment data and the time data are going to be the equal for all 2 cases.

As well as in chapter 2, the environment data does not considers any wind data and it is only based on a wave spectrum.

3.1.1. Environment data

The wave chosen is a White noise type which introduces a number of waves with frequencies uniformly distributed across an interval, and with the same amplitude direction. In the present cases the white noise spectra is used since we are mainly interested in the RAOs behavior of the platforms. Its features are (see Figure 39): amplitude 1m, 3 seconds shortest period, 20 seconds the longest and finally 40 wave's periods in 5 wave directions.

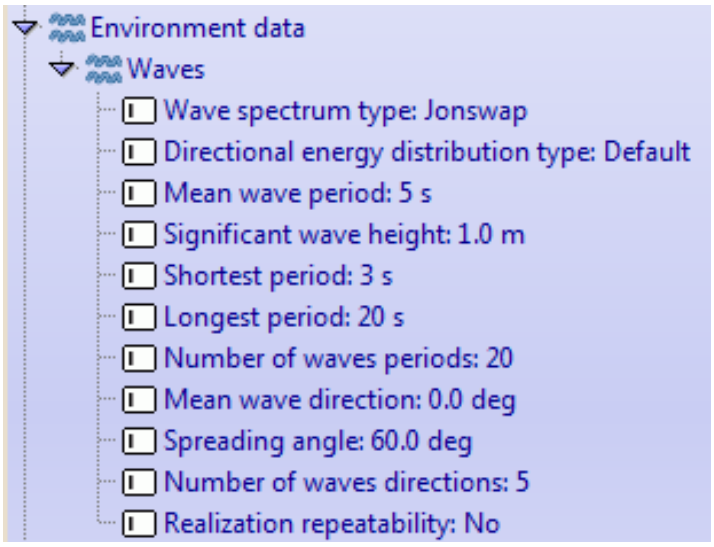

Figure 39. Enviroment data

3.1.2. Time data

On the other side; time data is also set (see Figure 40): simulation time 2300sec and start time recording 500sec. The parameters established for the simulation time and the step time are just introduced to the program for the sake of guidance because the SeaFEM internally evaluates optimal values for both them according to the analysis type.

Figure 40. Time data

3.1.3. Tdyn mooring lines creation

To create mooring lines all this parameters need to be set and introduced to the program in the following way:

```
set seg1 [TdynTcl_Create_Mooring_Segment body type xi yi zi xe ye ze w L A E S]
```

- **Body**: the index of the body which the mooring is linked to. In this study the body index is in all cases 1 because just one body is generated in each case.
- **Type**: determines the type of mooring segment to be used. Can be chosen between:
  - type= 1 – quasi-static elastic bar (spring able to work in both, tension and compression regimes).
  - type= 2 – quasi-static catenary
  - type= 3 – quasi-static cable (spring able to work only in tension).

- type= 4 – quasi-static elastic catenary.

In this study just the type 3, for the TLP, and the type 4, for the Spar Buoy, are to be used.

- **xi, yi, zi [m]:** are the fairleads x, y and z coordinates or also known as the mooring line initial point.
- **xe, ye, ze [m]:** are the anchor x, y and z coordinates or also known as the mooring line end point.
- **w [N/m]:** effective weight (actual weight minus buoyancy) per unit length. Sometimes it's presented as the effective mass [kg/m], then is just necessary to multiply that value per 9.81m/s^2 to get the effective weight.
- **L [m]:** length of the segment.
- **A [m^2]:** cross section area of the cable. Most times the diameter of the cable is given so it is not a difficult parameter to obtain.
- **E [Pa]:** Young modulus. Can be easily obtained by dividing the line extensional stiffness [N] by the cross section area of the cable [m^2].
- **S:** sea bed parameter. Having only effect when type 4 is chosen, can take several values.
  - **S=0:** catenary fixed to a seabed point.
  - **S=1:** considers a sandy bead contact.
  - **S=2:** considers a sliding seabed wire.
  - **S=3:** considers a sliding seabed chain.

In this project just seabed parameter 1 is used in the Spar Buoy floating structure.

3.2. Tension Leg Platform - Mooring analysis

The TLP mooring system is formed by 4 tension legs each duplicated and situated at a 27m radius from de structure center (see Table 12). In this kind of platform, the net equilibrating vertical force is supplied by vertical tension mooring cables secured by drilled-in anchors.

General			Geometry	
Nº Mooring Lines	8		**Depth to Anchors**	200 m
Angle	90 º		**Depth to Fairleads**	47.89 m
Other properties			**Radius to Anchor**	27 m
EML Mass Density	116.03	kg/m	**Radius to Fairleads**	27 m
EML Weight	1138.25	N/m	**Strech. ML Length**	151.73 m
EML Exten. Stiff.	1500000000	N	**ML Diameter**	0.127 m

Table 12. TLP mooring properties

3.3. Linear mooring lines case

The linear mooring lines case to be created consists of the same TLC script presented in the Chapter 2 at the TLP part of Geometry and properties. The only difference is that the Environment Data and the Time Data are changed as presented in the General Properties part from this chapter.

3.4. Non-linear mooring lines case.

This time the mooring lines stiffness matrix has to be removed from the original script and instead of it the mooring lines properties information is added to the program together with the other script information by attaching the following TLC script:

```
proc TdynTcl_CreateMooring { } {
          # quasi-static analysis
set seg1 [TdynTcl_Create_Mooring_Segment 1 3 27 0 -47.89 27 0 -200 1138.2546 151.73 0.01267 1.183898974E11 1]
set seg2 [TdynTcl_Create_Mooring_Segment 1 3 -27 0 -47.89 -27 0 -200 1138.2546 151.73 0.01267 1.183898974E11 1]
set seg3 [TdynTcl_Create_Mooring_Segment 1 3 0 27 -47.89 0 27 -200 1138.2546 151.73 0.01267 1.183898974E11 1]
set seg4 [TdynTcl_Create_Mooring_Segment 1 3 0 -27 -47.89 0 -27 -200 1138.2546 151.73 0.01267 1.183898974E11 1]
set seg5 [TdynTcl_Create_Mooring_Segment 1 3 27 0 -47.89 27 0 -200 1138.2546 151.73 0.01267 1.183898974E11 1]
set seg6 [TdynTcl_Create_Mooring_Segment 1 3 -27 0 -47.89 -27 0 -200 1138.2546 151.73 0.01267 1.183898974E11 1]
set seg7 [TdynTcl_Create_Mooring_Segment 1 3 0 27 -47.89 0 27 -200 1138.2546 151.73 0.01267 1.183898974E11 1]
set seg8 [TdynTcl_Create_Mooring_Segment 1 3 0 -27 -47.89 0 -27 -200 1138.2546 151.73 0.01267 1.183898974E11 1]
        TdynTcl_Message "TdynTcl_CreateMooringLine finished!!!" notice
}
```

And finally, the 4 duplicated mooring lines are created (see Figure 41).

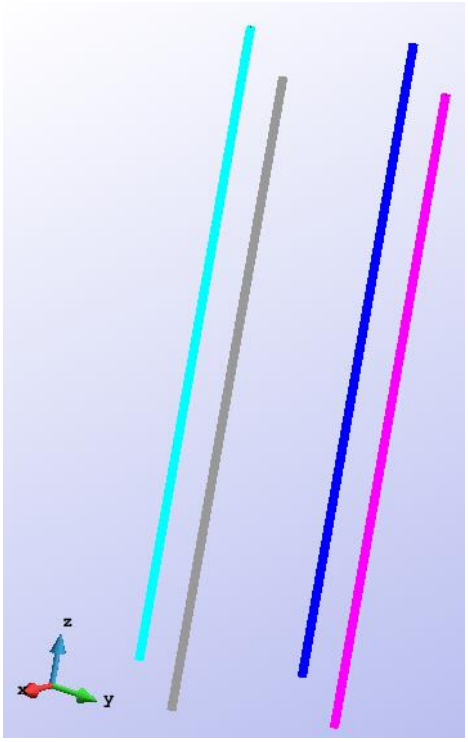

Figure 41. TLP mooring lines created

3.5. Motion results comparison

Once both cases are created, the motion result comparison is done. All results have been gathered in the following graphs: first of all surge results (see Figure 42), followed by heave results (see Figure 43) and finally the pitch results (see Figure 44) in a time scale.

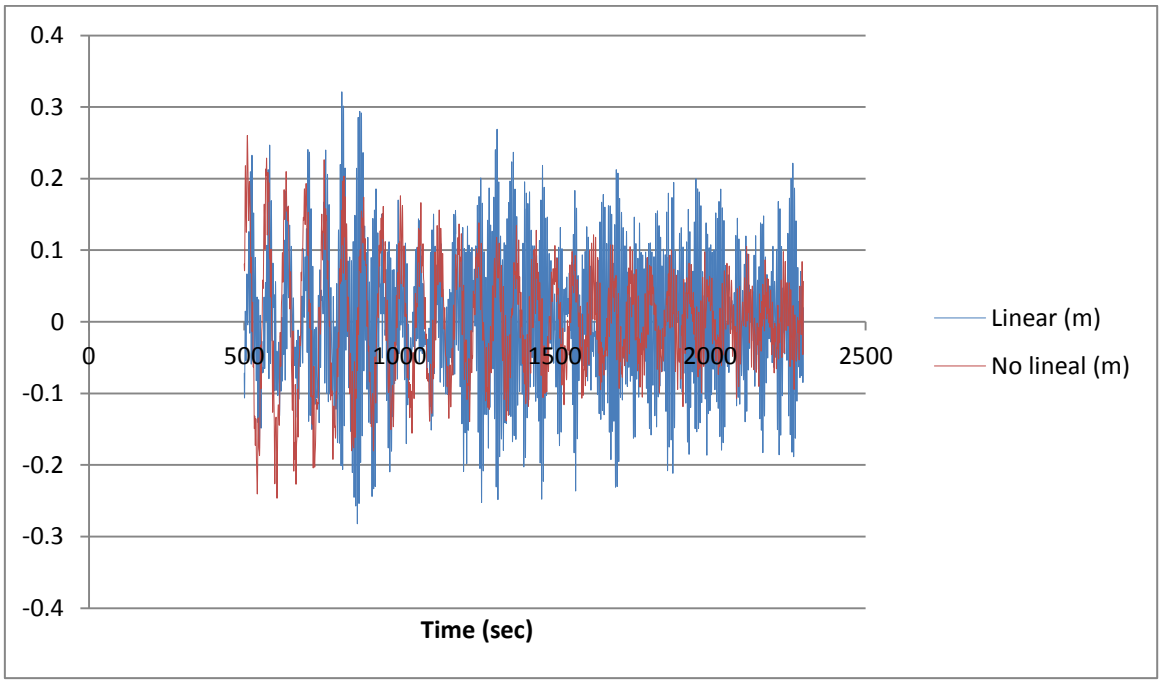

Figure 42. TLP Surge motion results comparison

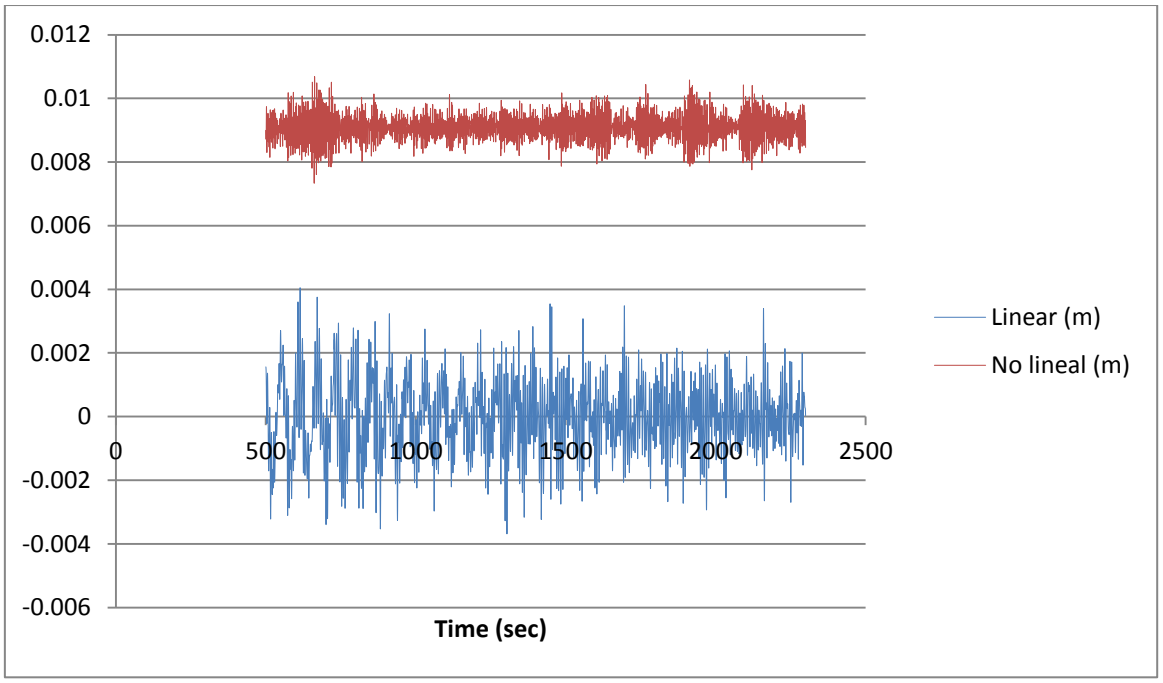

Figure 43. TLP Heave motion results comparison

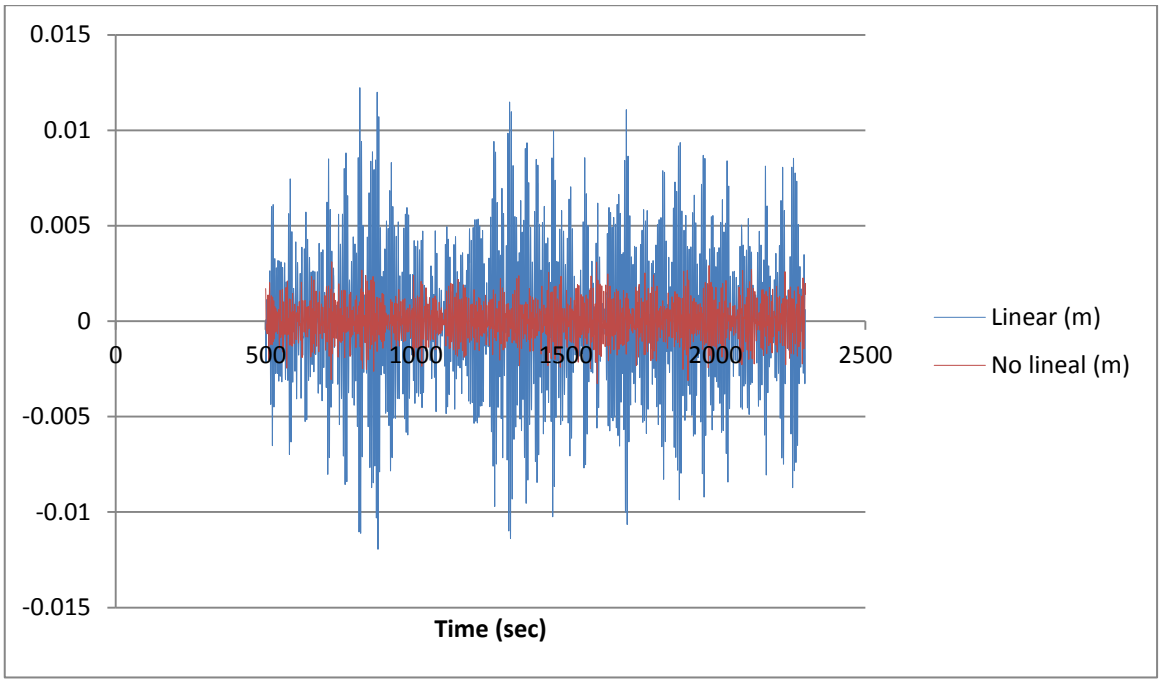

Figure 44. TLP Pitch motion results comparison

At first sight all those platform motion results seem to be logical because the displacements keep into rational dimensions with the waves induced. Furthermore, as explained at this chapter introduction, the displacements results to be obtained from these different mooring ways of study are not supposed to be the similar and actually there are not too many differences between them.

At last, comment that though the heave displacements results with the non-linear results are slightly higher than the ones obtained with the linear results, the difference is considered insignificant because is just by 1cm.

3.6. Spar-Buoy - Mooring analysis

The Spar-Buoy mooring system is formed by 3 catenary lines at 120º one from each other attached to the Spar at 70m below the SWL (see Table 13). It actually consists on several pre-tensioned anchor lines arrayed to the structure in order to keep it in the desired location.

General			Geometry	
Nº Mooring Lines	3		**Depth to Anchors**	-320 m
Angle	120	º	**Depth to Fairleads**	-70 m
Other properties			**Radius to Anchor**	5.2 m
EML Mass Density	77.71	kg/m	**Radius to Fairleads**	853.9 m
EML Weight	762.3351	N/m	**Unstr. ML Length**	902.2 m
EML Exten. Stiff.	384200000	N	**ML Diameter**	0.09 m

Table 13. Self-Buoy mooring properties

3.7. Linear mooring lines case

Starting from the Spar-Buoy programme created in Chapter 2, the Environment Data and the Time Data is to be actualized to the one set in the General Properties part at the beginning of this chapter. The linear mooring lines case to be created uses the same TLC script than the Spar-Buoy program too. In which the mooring lines are introduced to it by a mooring stiffness matrix.

3.8. Non-linear mooring lines creation

The mooring lines properties information is added to the program together with the following TLC script (notice that must be removed the lineal mooring stiffness matrix from the original TLC script):

```
proc TdynTcl_CreateMooring { } {
          # quasi-static analysis
set seg1 [TdynTcl_Create_Mooring_Segment 1 4   5.2 0 -70 853.9 0 -320 698.094 902.2 0.006362  6.039657E+10 1]
set seg2 [TdynTcl_Create_Mooring_Segment 1 4  -2.6 4.5 -70 -426.95 739.5 -320 698.094 902.2 0.006362  6.039657E+10 1]
set seg3 [TdynTcl_Create_Mooring_Segment 1 4   -2.6 -4.5 -70 -426.95 -739.5 -320 698.094 902.2 0.006362  6.039657E+10 1]
        TdynTcl_Message "TdynTcl_CreateMooringLine finished!!!" notice
}
```

And finally these are the mooring lines created (see Figure 45):

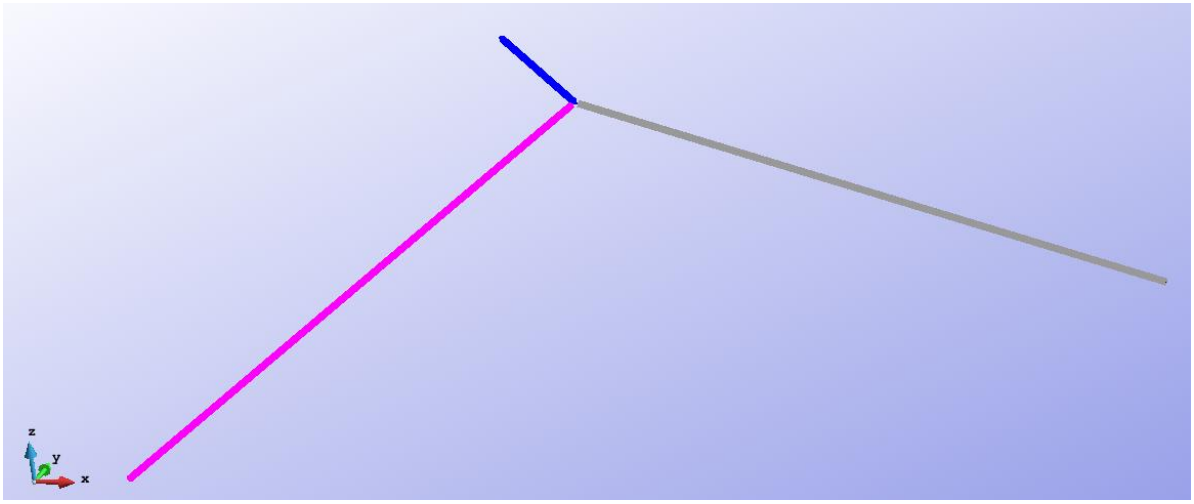

Figure 45. Spar-Buoy created mooring lines

When trying to run this case, heave results obtained were not by far the ones expected, because the non-linear heave displacements acquired results shown that the body was in its equilibrium position at 5 meters below the sea water line. This particular factor can be attributed to many different causes:

- The mesh is not the optimal one so that the body properties are slightly modified.

- Or as in this case, the non-linear mooring lines created produce an extra -1600000N vertical force to the body. This extra force is the equivalent to the extra 3 lines weight that have been developed.

In order to solve this basic equilibrium problem this external load is summed as one external force more in the body properties (see Figure 46). And it is checked that now the body is in vertical equilibrium.

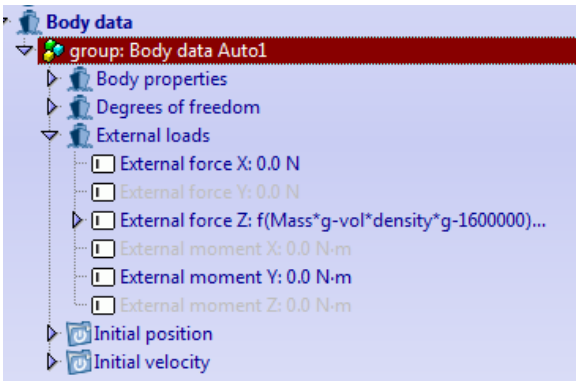

Figure 46. Spar-Buoy modified body data

3.9. Motion results comparison

Having created both analysis cases, it is proceeded with the motion results comparison and above are shown all the results graphs: first the surge (see Figure 47), then the heave (see Figure 48) and finally the pitch results (see Figure 49) in a time scale.

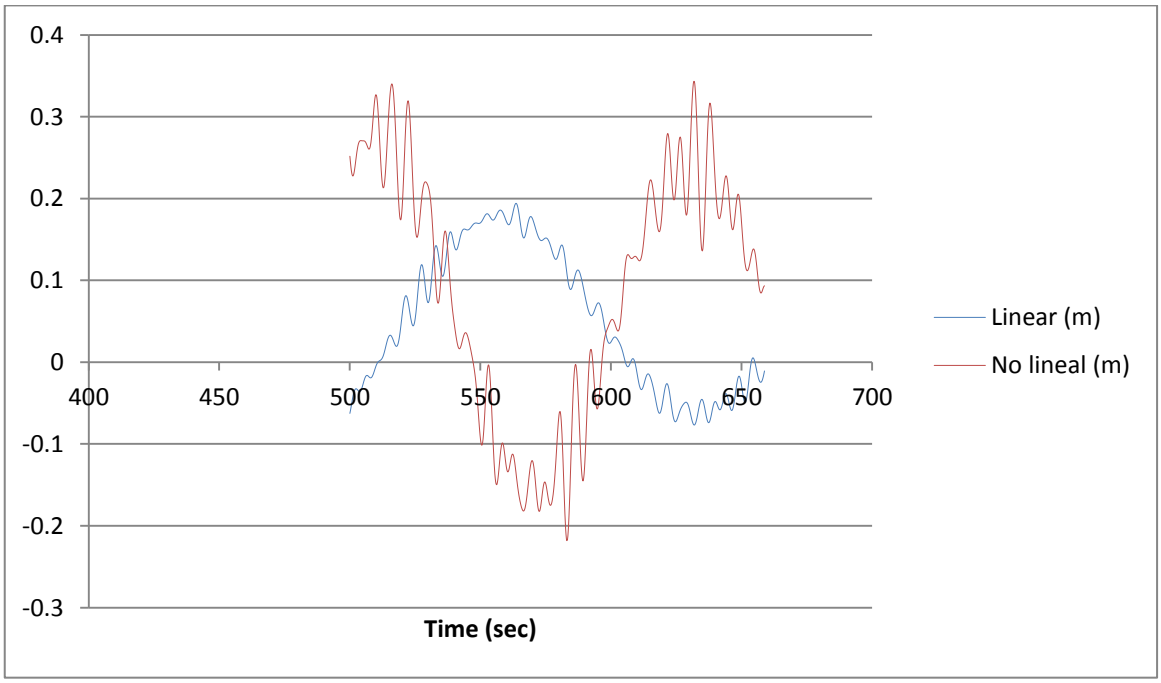

Figure 47. Spar-Buoy Surge motion results comparison

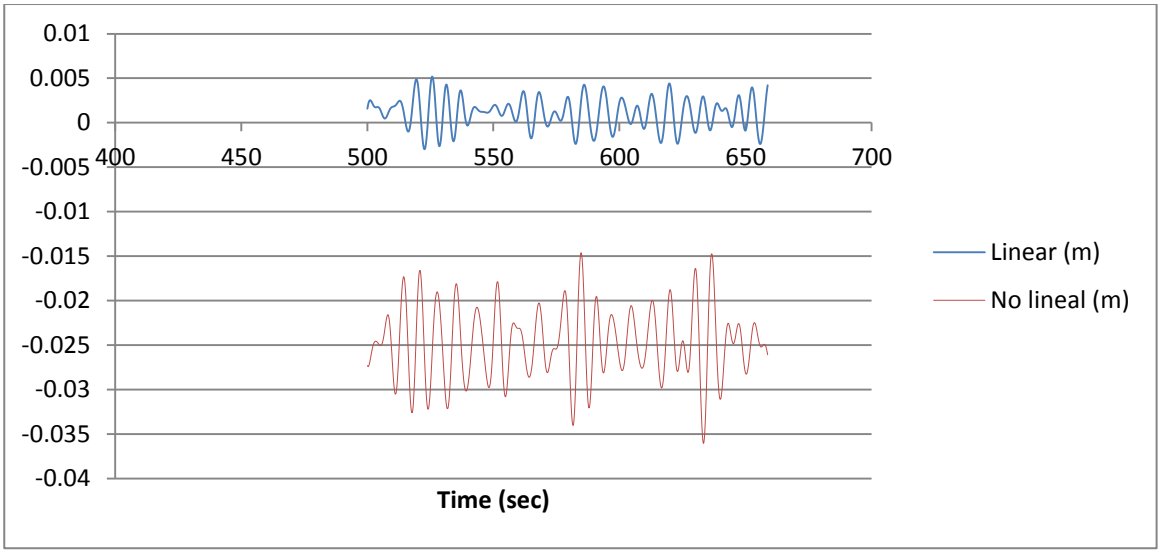

Figure 48. Spar-Buoy Heave motion results comparison

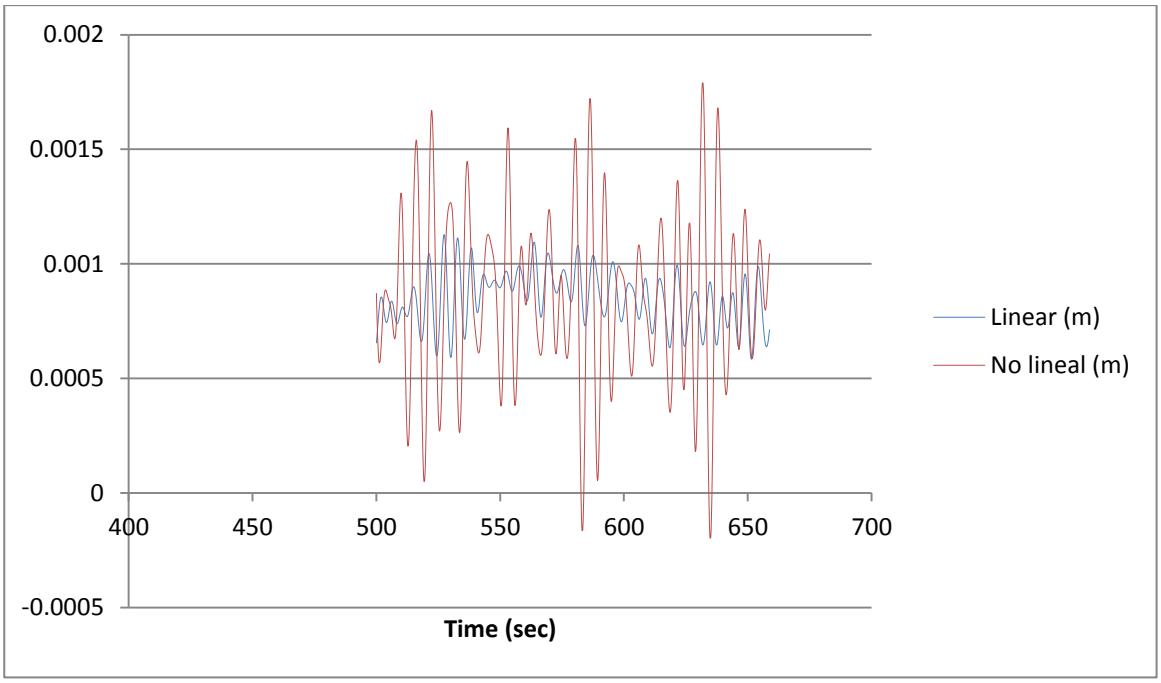

Figure 49. Spar-Buoy Pitch motion results comparison

As a final point, it can be concluded that all displacements obtained are really closed ones to the others in both linear and non-linear mooring lines created. Although little differences can be noticed between the surge, heave and pitch results they are considered as negligible being them attributed to the variances between the linear and the non-linear formulation.

3.10. Mooring forces comparison

On this lasts Chapter's 3 part, the mooring forces produced to the studied platforms analysis is to be done.

3.11. TLP mooring forces obtained

As being Fy and Mx and Mz results equal to 0 (due to the freedom degrees set), here are just shown and analysed Fx, Fz and My results graphs.

On the X direction forces –Fx – (see Figure 50) a tendency to decrease as time passes can be clearly observed. The medium forces resulting are equal to ±20000N which could be considered as a possible result magnitude. Furthermore the Fx magnitude and sign varies from negative to positive values as a possible wave direction result.

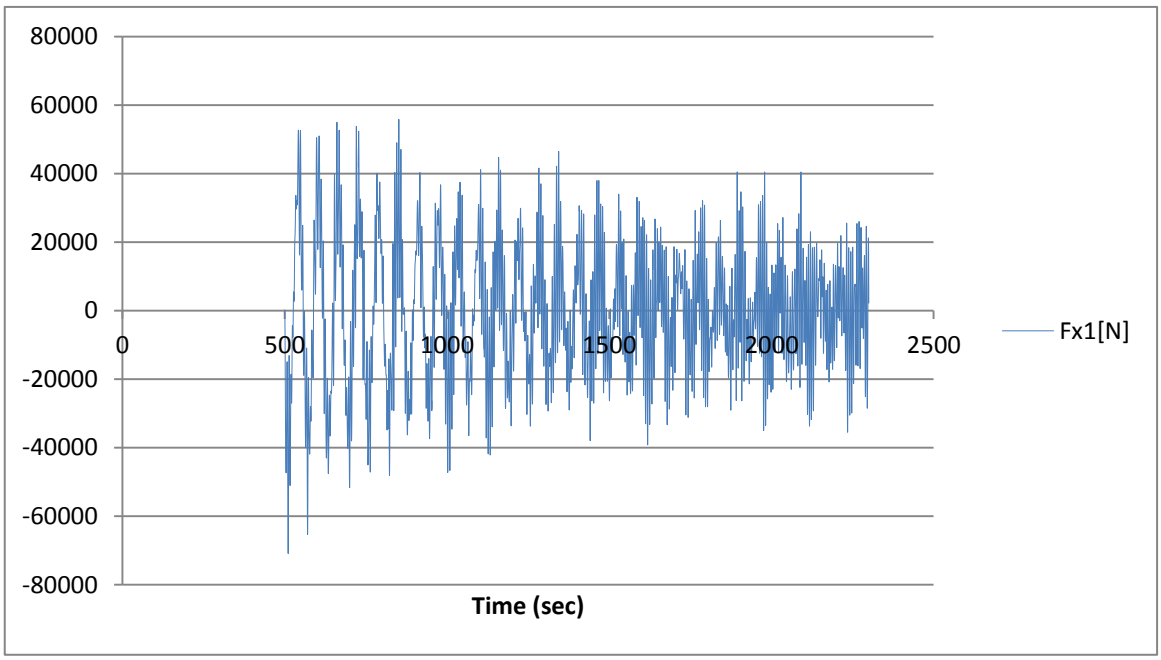

Figure 50. Obtained Fx TLP mooring line

On the other side, the Z direction forces –Fz– (see Figure 51) results obtained show up that the mooring lines are at all time in tension pulling down the TLP as it should be due to its basic conception theory.

The medium Fz force obtained is about -2.94E+07N which is actually a possible and reasonable magnitude value to be expected from these mooring lines.

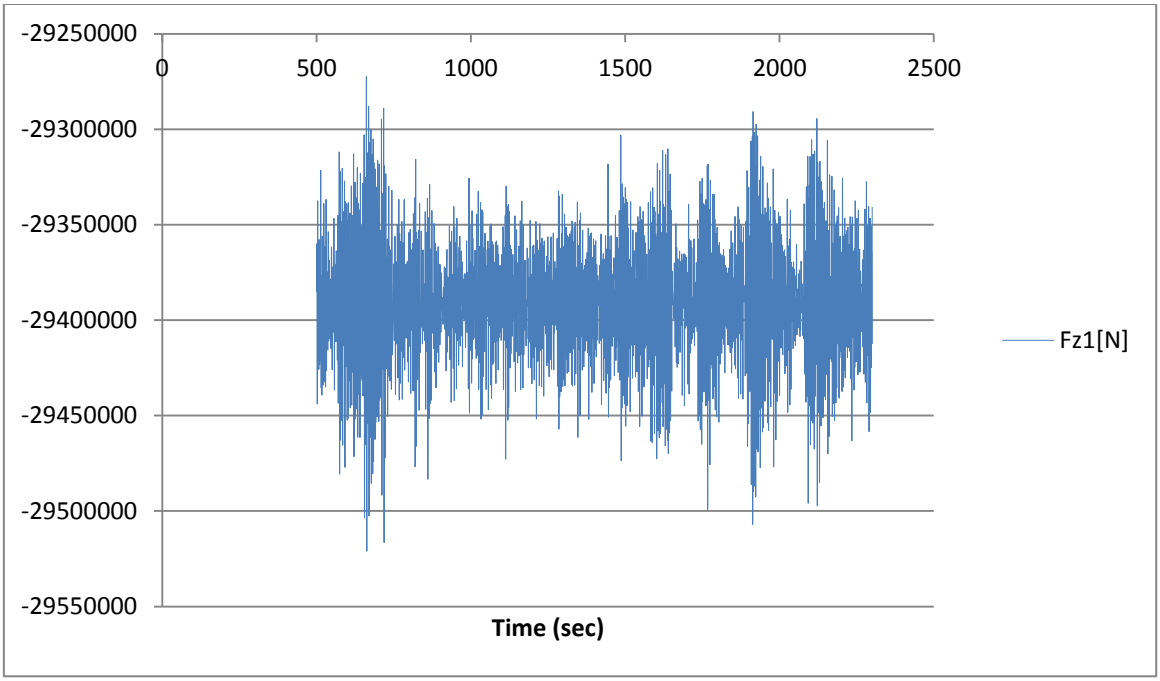

Figure 51. Obtained Fz TLP mooring line

To conclude with the TLP forces transmitted by its mooring lines, the Moment on Y –My – (see Figure 52) is obtained. Being it all centred at the origin it can be concluded that these moments are equilibrated by the same mooring lines which create them.

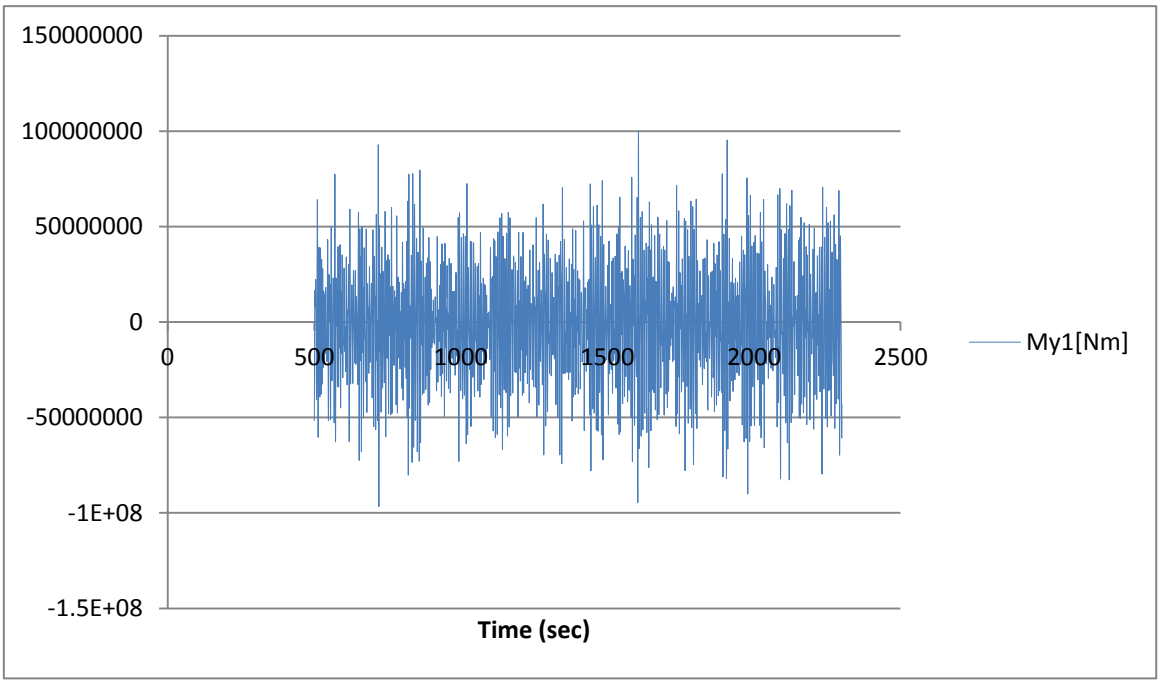

Figure 52. Obtained My TLP mooring line

3.12. Spar-Buoy mooring forces obtained

As well as with the TLP, just Fx, Fz and My are shown due to the null values obtained for the other forces and moments because the freedom degrees set on the numerical model creation.

The achieved X direction forces –Fx – (see Figure 53) values show a clear tendency to stabilization around the 0N force by shrinking as time developments its peak values.

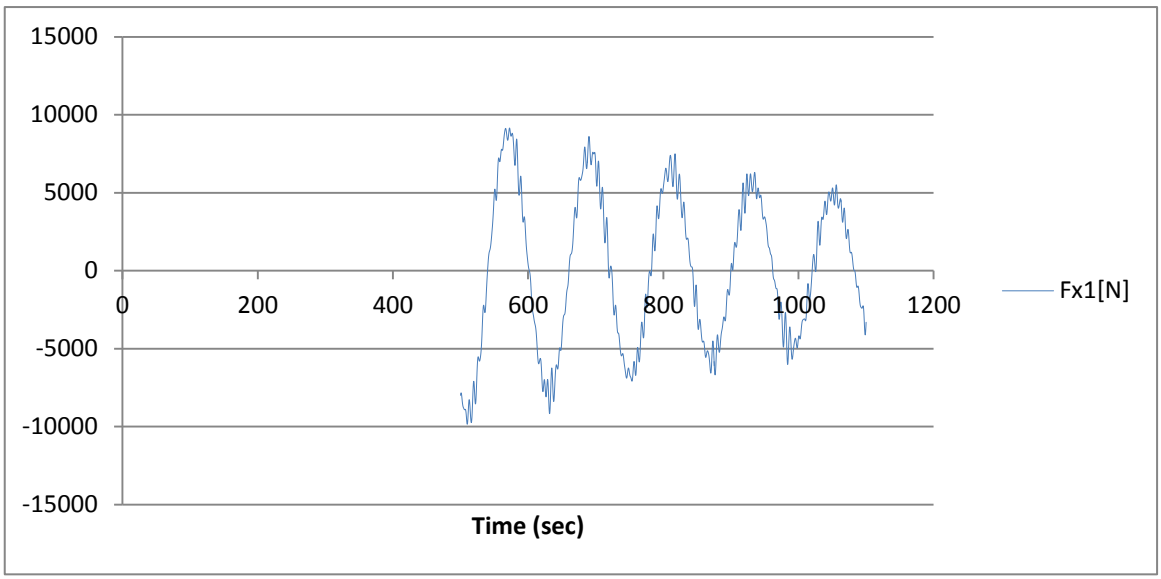

Figure 53. Obtained Fx Spar-Buoy mooring line

As well as Fx, the Z direction forces –Fz – (see Figure 54) also tend to stabilize to -1607925N. This force could be considered as correct due to its reasonable magnitude and its negative sign which shows that the mooring lines are transmitting a vertical negative (pulling) force to the Spar-Buoy structure.

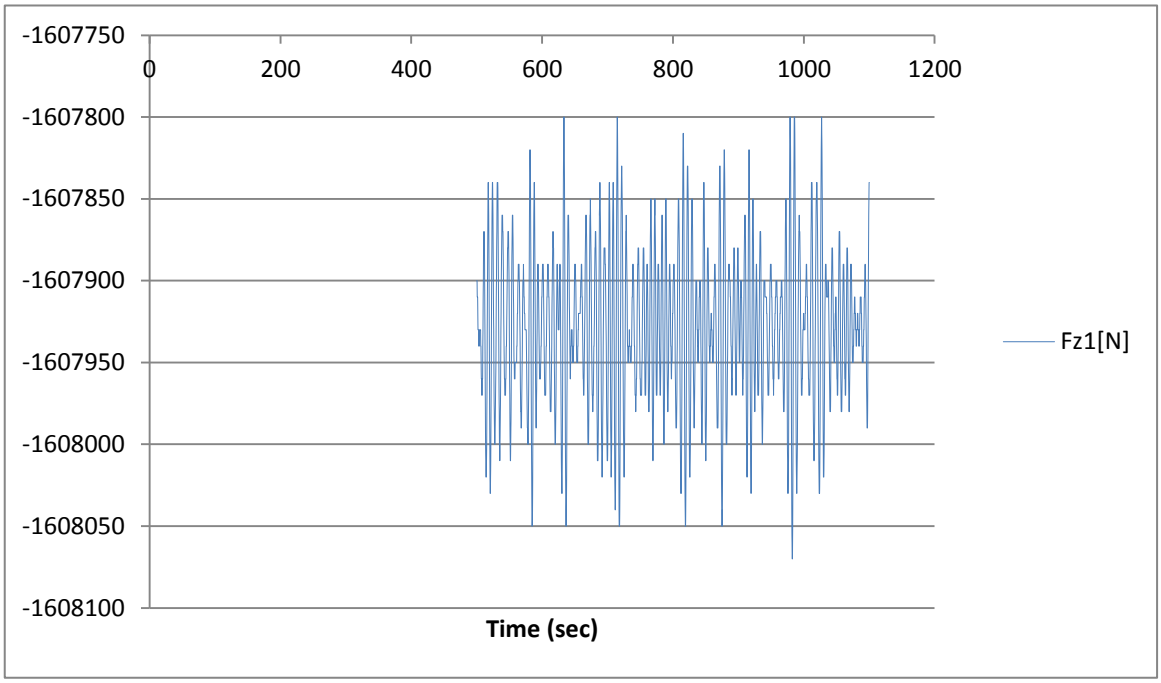

Figure 54. Obtained Fz Spar-Buoy mooring line

As the last result obtained, the moment on Y –My – (see Figure 55) is presented. This also tends to become stabilized although this case not to the 0Nm, thought to the approximated -100000Nm which would produce a constant moment on Y to the structure.

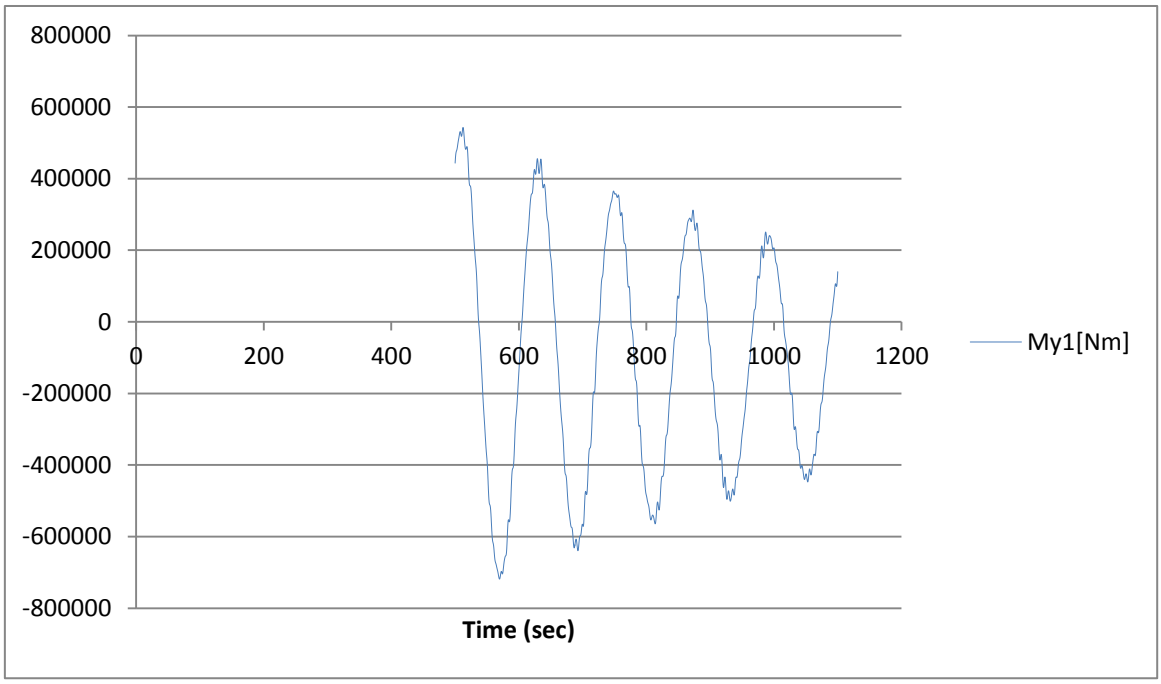

Figure 55. Obtained My Spar-Buoy mooring line

As clear tendencies are noticed in all the graphs obtained this time the computational time has been reduced to 1100 seconds.

Chapter 4. Conclusions

4.1. RAO results

For both two floating structure studied, the Tension Leg Platform and the Self-Buoy, accurate RAO results were obtained being this a transcended inflection point to the total project work because it was the best confirmation which could have been obtained in order to enable going forward with the next project steps.

4.2. Displacements linear vs non-linear

Following the RAO results calculus, a comparison between the linear and non-linear displacements results had to be done by creating new study cases based on the ones created before. Although the procedure to get this done was not a complex procedure, some little handicaps were found between the linear vs non-linear formulation. The uppermost importance which needs to be given to the vertical platforms equilibrium (mainly when changing from linear to non-linear mooring lines procedure because an important extra weight and loads are applied to the model) was really emphasized.

As expected there where slightly differences between linear and non-linear results obtained but as it has already been said, there were predictable from the first beginning.

4.3. Mooring forces

Finally, the mooring forces analysis is done. From the obtained forces which the mooring lines created to the body it can be concluded that TLP platforms induced forces are more stabilized and constant than the forces which the Spar-Buoy platform suffers. Unfortunately those variant forces are the ones which make the Spar-Buoy structure suffer much more fatigue load effects.

4.4. Programing

As explained through the project, the SeaKeeping program is used. Thought it is a really powerful tool, once finished the whole procedure and programing tasks, can be undoubtedly admitted that lots of experience and knowledge is actually needed when working with this kind of programs.

This lack of programing practice and the basically none offshore structures previous knowledge have been the main handicap during the entire project.

Although in this project the complete procedures have been resumed into some pages, the principal and may be 80% of the total work and time invested in the project has been spent between programing and searching for information.

Many other figures could have been added in this project thought it was considered that here there are the ones most significant to the study objectives.

4.5. Dedication and human factor

This Project started at the beginning of November 2013 and has actually finished at the beginning of July 2014. At the beginning the work rhythm was really slow, and a really long and ponderous period of time was invested for getting really into the offshore platforms subject. Many articles and books were musts to be read just in order to get in that so extensive an innovative world.

Not until the beginning of December the study object floating platforms were firmly stated. Since, then an arduous most concrete investigation process was taken up.

Since then a defeating and sometimes overwhelming - all at the same time - periods where ongoing due to the really essential knowledge needed to succeed in this so complex calculus procedures.

Actually the most difficult fact was when discerning if results were optimal or not due to the huge understanding essential to produce these verdicts.

To conclude state that an 8 month period of independent learning is not enough to deepen enough to this so wide topic of the offshore platforms. Although it has not been as complete as pretended many new concepts (like equations of motions, RAOs, programing…) have been assumed and are going to be useful to myself in the near future.

Bibliography

References:

[1] http://unfccc.int/resource/docs/convkp/kpeng.pdf

[2] http://www.4-power.eu/media/3109/offshore-wind-guide-june-2013.pdf

[3] http://www.mpoweruk.com/energy_resources.htm#costs

[4] P 26. Parametric Design of Floating Wind Turbines Christopher Tracy B.S Mechanical Engineering Rice University, 2001

[5] http://www.houston-offshore.com/solutions/tension-leg-platform/

[6] https://www.rigzone.com/training/insight.asp?insight_id=305&c_id=12

[7] http://www.nrel.gov/docs/fy10osti/45891.pdf

[8] Pag 74: http://www.compassis.com/downloads/Manuals/SeaFEMTutorials.pdf

[9] http://www.wpi.edu/Pubs/E-project/Available/E-project-030411-161930/unrestricted/MQP_Final_Report_03_09_2011.pdf

[10] http://www.ewea.org/fileadmin/ewea_documents/documents/publications/WD/2009_december/Science_corner_-_December_2009.pdf

[11] http://www.ijose.org/sub/issues/pdf/vol34/A%20Study%20on%20Mooring%20System%20Design%20of%20Floating%20Offshore%20Wind%20Turbine%20in%20Jeju%20Offshore%20Area.pdf

[12] http://www.nrel.gov/docs/fy10osti/47535.pdf

[13] http://www.nrel.gov/docs/fy13osti/58098.pdf

All web pages were consulted before the 01/07/2014

General bibliography:

- Matha, D., "Modal Development and Loads Analysis of an Offshore Wind Turbine on a Tension Leg Platform, with a Comparison to Other Floating Turbine Concepts", Thesis, Ph.D., NREL, April 2009.
- SeaFEM user manual.

Annex 1 – Equations of motion and RAO

What a model is? A model is a mathematic representation of a system. Generally it can be characterized by ODEs. Being ODEs really difficult to solve, the lineal ones are the easiest.

Knowing that a system is being formed by several interrelated and detachable elements from its surroundings for its analysis, we can consider our system and its components to be:

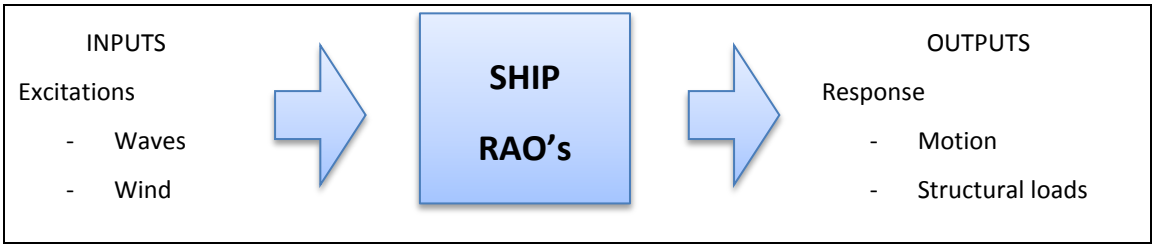

In this case the response to be studied is to be the motion response on its six degrees of freedom (see Figure 56).

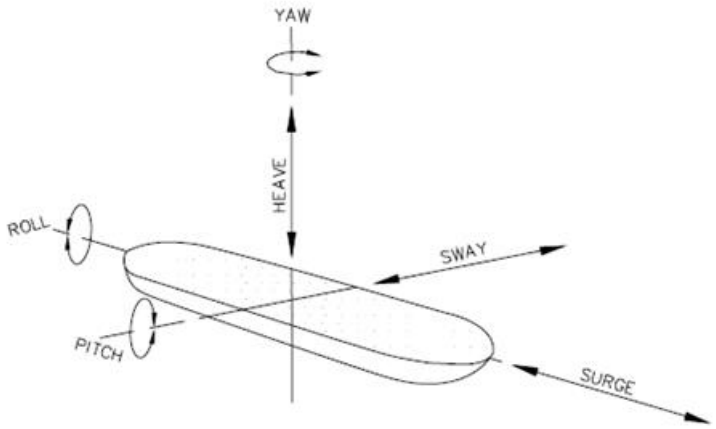

Figure 56. Ships degrees of freedom.
Source: http://www.corpsnedmanuals.us/

Based on the equation of movement governing the rigid-body motions of a floating body (see Equation 1 and Equation 2), which consists of standard Newtonian equations of motion describing the 6 modes of motion, the ship response to its inputs can be obtained.

Equation 1

$$(M_{added}(w) + M_{WT} + M_{str})\ddot{\zeta}(t) + (B_{WT} + B_{str}(w))\dot{\zeta}(t) + \left(C_{WT} + C_{str} + C_{mooring}\right)\zeta(t) = y(w)$$

Equation 2

$$M_{total}(w)\ddot{\zeta} + B_{total}(w)\dot{\zeta} + C_{total}(w)\zeta = y(w)$$

Where;

$\boldsymbol{M_{added}}$ is the added mass matrix

$\boldsymbol{M_{WT}}$ is the mass matrix of the wind turbine at a constant wind speed

$\boldsymbol{M_{str}}$ is the mass matrix of the platform

$\boldsymbol{B_{WT}}$ is the damping matrix of the wind turbine

$\boldsymbol{B_{str}}$ is the damping matrix of the platform

$\boldsymbol{C_{WT}}$ is the stiffness matrix of the wind turbine

$\boldsymbol{C_{str}}$ is the stiffness matrix of the platform

$\boldsymbol{C_{mooring}}$ is the stiffness matrix of the mooring system

$\ddot{\boldsymbol{\zeta}}, \dot{\boldsymbol{\zeta}}, \boldsymbol{\zeta}$ are acceleration, velocity and displacement of the system.

When solving ODEs, as the equation of motions, we can carry on in two different ways: in the time domain or in the frequency domain.

- In the time domain all inputs and outputs are functions of time and so we are actually getting the time history of the motion for an only given frequency, whereas
- in the frequency domain al this inputs and outputs are function of complex angular frequency and so we get solutions for the motion amplitude over a range of frequencies.

To work in the frequency domain the Laplace transformation is required; furthermore it gives another functional description that often simplifies the analysing process of the performance of the system. The Laplace transformation of this system (see Equation 3) goes as follows:

Equation 3

$$-\boldsymbol{w^2 M_{total}(w)X(w)} + \boldsymbol{iwB_{total}(w)X(w)} + \boldsymbol{C_{total}(w)X(w)} = \boldsymbol{Y(w)}$$

The full aim of calculating the body motions – in this project – is to find out the bodies behaviour into its characteristic frame conditions in order to determine if there is any risk to get into the structure natural frequencies.

- Natural frequencies are the frequencies at which a system would tend to oscillate if it happened to be lack of any driving or damping force. Natural vibration is the consequence of the free vibrations of any elastic body.
- If there chanced to appear natural vibrations as well any forced vibration – due to an applied force – at any of the natural frequencies, the body amplitude of vibration would increase assorted getting itself into a resonance effect.

The natural frequencies in each of the six degrees of freedom can be obtained with the following equation (see Equation 4):

Equation 4

$$w_{n_i} = \sqrt{\frac{C_{total}}{M_{total}}}$$

To define the magnitude and the phase of a floating structure's response to the sea conditions it is comes necessary to obtain it's the RAO's function. The RAO or also known as the Response Amplitude Operator gives information about the performance of a floating structure when operating at sea. That is, the floating body response on a given mode of motion due to a unit amplitude wave as a function of frequency.

In fact, solving the equation of motion in the frequency domain, the RAO for each of the six modes of motion is obtained (see Equation 5).

Equation 5

$$\frac{X(w)}{-w^2 M_{total}(w) + iwB_{total}(w) + C_{total}(w)} = \begin{bmatrix} RAO_1(w) \\ RAO_2(w) \\ RAO_3(w) \\ RAO_4(w) \\ RAO_5(w) \\ RAO_6(w) \end{bmatrix}$$

From the above equation, it is clear that RAOs are complex in nature. The real and imaginary parts give the magnitude and the phase of the RAO. If RAO in one direction is x + iy, then (see Equation 6):

Equation 6

$$Magnitude\ of\ RAO = \sqrt{x^2 + y^2}$$

$$Phase\ of\ RAO = arctan\left(\frac{y}{x}\right)$$